Few-Body Systems manuscript No.
(will be inserted by the editor)

N.V. Shevchenko

Three-body antikaon-nucleon systems

arXiv:1608.06126v2 [nucl-th] 3 Nov 2016

Received: date / Accepted: date

Abstract The paper contains a review of the exact or accurate results achieved in the field of the three-body antikaon-nucleon physics. Different states and processes in $\bar{K}NN$ and $\bar{K}\bar{K}N$ systems are considered. In particular, quasi-bound states in K^-pp and K^-K^-p systems were investigated together with antikaonic deuterium atom. Near-threshold scattering of antikaons on deuteron, including the K^-d scattering length, and applications of the scattering amplitudes are also discussed.

All exact three-body results were calculated using some form of Faddeev equations. Different versions of $\bar{K}N$, ΣN, $\bar{K}\bar{K}$, and NN potentials, specially constructed for the calculations, allowed investigation of the dependence of the three-body results on the two-body input. Special attention is paid to the antikaon-nucleon interaction, being the most important for the three-body systems. Approximate calculations, performed additionally to the exact ones, demonstrate accuracy of the commonly used approaches.

Keywords Few-body exotic systems · AGS equations · Antikaon-nucleon interaction

Contents

1 Introduction . . . 2
2 Two-body interactions . . . 3
2.1 Antikaon-nucleon interaction, experimental data . . . 4
2.2 Phenomenological and chirally motivated $\bar{K}N$ potentials . . . 6
2.3 Nucleon-nucleon and $\Sigma N(-\Lambda N)$ potentials . . . 9
2.4 Antikaon-antikaon interaction . . . 10
3 AGS equations for coupled $\bar{K}NN - \pi\Sigma N$ and $\bar{K}\bar{K}N - \bar{K}\pi\Sigma$ channels . . . 11
4 Quasi-bound states . . . 12
4.1 Two ways of a quasi-bound state evaluation . . . 12
4.2 K^-pp quasi-bound state: results . . . 14
4.3 K^-pp quasi-bound state: comparison to other results . . . 15
4.4 K^-d quasi-bound state . . . 17
4.5 $\bar{K}\bar{K}N$ system: results . . . 17
5 Near-threshold K^-d scattering . . . 18
5.1 Methods and exact results . . . 18
5.2 Approximate calculations and comparison to other results . . . 19
6 $1s$ level shift of kaonic deuterium . . . 21
6.1 Approximate calculation of kaonic deuterium $1s$ level . . . 21
6.2 Exact calculation of kaonic deuterium: Faddeev equations with Coulomb interaction . . . 22
6.3 Exact calculation of kaonic deuterium: results . . . 23
7 Summary . . . 25

The work was supported by the Czech CACR grant 15-04301S.

N.V. Shevchenko
Nuclear Physics Institute, 25068 Řež, Czech Republic
E-mail: shevchenko@ujf.cas.cz

1 Introduction

An interest to the exotic systems, which consist of antikaons and nucleons, rose recently after the statement [1; 2], that deep and narrow quasi-bound states can exist in $\bar{K}NN$ and $\bar{K}NNN$ systems. Due to this, several calculations of the quasi-bound state in the lightest $\bar{K}NN$ system with $J^P = 0^-$ quantum numbers, that is K^-pp, were performed. Among all calculations those using Faddeev-type equations are the most accurate ones. The first results of the two accurate calculations [3; 4; 5] confirmed the existence of the quasi-bound state in the K^-pp, but the evaluated binding energies and widths are far different from those predicted in [1; 2]. The results of the two groups [3; 4; 5] also differ one from the other, and the main reason for this is a choice of the antikaon-nucleon interaction, being an input for the three-body calculations.

The question of the quasi-bound state in the K^-pp system is far from being settled from experimental point of view as well. The first experimental evidence of the K^-pp quasi-bound state existence occurred in the FINUDA experiment [6] at the DAΦNE e^+e collider. Recently performed new analyses of old experiments, such as OBELIX [7] at CERN and DISTO [8] at SATURNE also claimed the observation of the state. However, there are some doubts, whether the observed structure corresponds to the quasi-bound state. The experimental results also differ from each other, moreover, their binding energies and widths are far from all theoretical predictions. Since the question of the possible existence of the quasi-bound state in the K^-pp system is still highly uncertain, new experiments are being planned and performed by HADES [9] and LEPS [10] Collaborations, and in J-PARC E15 [11] and E27 [12] experiments.

It was demonstrated [4] that the $\bar{K}N$ interaction plays a crucial role in the $\bar{K}NN$ calculations. It is much more important than the nucleon-nucleon one, but is far less known. Therefore, a model of the antikaon-nucleon interaction, which is more accurate in reproducing experimental data than that from [3; 4], was necessary to construct. The experimental data on $\bar{K}N$ interaction, which can be used for fitting parameters of the potential, are: near-threshold cross-sections of K^-p scattering, their threshold branching ratios, and shift and width of $1s$ level of kaonic hydrogen (which should be more accurately called "antikaonic hydrogen"). The last observable has quite interesting experimental history and finally was measured quite accurately. As for the theoretical description of kaonic hydrogen, many authors used approximate Deser-type formulas, which connect $1s$ level shift of an hadronic atom with the scattering length, given by strong interaction in the pair. The question was, how accurate are the approximate formulas, derived for the pion-nucleon interaction, for the antikaon-nucleon system. It was demonstrated in [13; 14] and later in [15] that Deser-type formulas has low accuracy for the antikaon-nucleon system.

Another question of antikaon-nucleon interaction is a structure of the $\Lambda(1405)$ resonance, which couples the $\bar{K}N$ system to the lower $\pi\Sigma$ channel. $\Lambda(1405)$ is usually assumed as a quasi-bound state in the higher $\bar{K}N$ channel and a resonance state in the lower $\pi\Sigma$ channel. But it was found in [16] and later in other papers that a chirally motivated model of the interaction lead to a two-pole structure of the resonance. Keeping these two points of view in mind, two phenomenological $\bar{K}N$ potentials with one- and two-pole structure of the $\Lambda(1405)$ resonance were constructed in [14]. Their parameters were fitted to the experimental data, and $1s$ level shift and width of kaonic hydrogen were calculated directly, without any approximate formulas.

It turned out [14] that it is possible to construct phenomenological potentials with one- and two-pole $\Lambda(1405)$ resonance which describe existing low-energy experimental data with the same level of accuracy. Due to this, the two $\bar{K}N$ potentials were used as an input in calculations of the low-energy elastic K^-d scattering in [17]. But after the publication of the K^-d results, SIDDHARTA collaboration reported results of their measurement of kaonic hydrogen characteristics [18]. The results turned out to be quite different from the previously measured results of DEAR experiment [19] and compatible with older KEK data [20]. Due to this, the $\bar{K}N$ potentials were refitted in such a way, that they reproduce the most recent experimental data on the $1s$ level shift and width of kaonic hydrogen. The calculations of the low-energy elastic kaon-deuteron scattering were repeated in [21] with the new potentials. In addition, an approximate calculation of the $1s$ level shift and width of kaonic deuterium was performed. It was done approximately using a complex $K^- - d$ potential, reproducing the elastic three-body K^-d amplitudes.

It was found that the three-body K^-d system also does not allow to make preference to one of the two phenomenological $\bar{K}N$ potentials and by this to solve the question of the number of $\Lambda(1405)$ poles.

In order to support the statement, one more, a chirally motivated $\bar{K}N$ potential was constructed. As other chiral models, it has two poles forming the $\Lambda(1405)$ resonance. Parameters of this potential were also fitted to the low-energy experimental data on K^-p scattering and kaonic hydrogen, the chirally motivated $\bar{K}N$ potential reproduces all antikaon-nucleon data with the same accuracy as the two phenomenological models.

Another way of investigation of the $\Lambda(1405)$ resonance was suggested and realised in [22], were low-energy breakup of the K^-d system was considered. The idea was that the resonance should be seen as a bump in so called deviation spectrum of neutrons in the final state of the reaction. However, $\Lambda(1405)$ is so broad that it was seen as a bump in some cases only.

Finally, the calculations of the three-body $\bar{K}NN$ system with different quantum numbers were repeated in [23; 24] using all three models of the $\bar{K}N$ interaction. In particular, the binding energy and width of the K^-pp quasi-bound state were evaluated, the low-energy K^-d amplitudes were calculated and the $1s$ level shift and width of kaonic deuterium were predicted. A search of the quasi-bound state in the K^-d system was also performed, but the results are negative.

After the approximate calculations of the characteristics of deuterium, the exact calculations were performed in [25]. Namely, Faddeev-type equations with strong plus Coulomb interactions, suggested in [26], were solved. It was the first time, when the equations [26], initially written and used for a system with Coulomb interaction being a correction to a strong potential, were used for investigations of an hadronic atom, where Coulomb potential plays the main role. Since the equations are much more complicated than "usual" AGS ones (containing short-range potentials only), the calculations were performed with simple complex $\bar{K}N$ potentials, reproducing only some of the experimental K^-p data. Comparison of the dynamically exact three-body results with the previous approximate ones shown that the approximation of the kaonic deuterium as a two-body system is quite accurate for this task.

Another three-body exotic system, consisting of two antikaons and one nucleon, was studied in [27]. It was expected that a quasi-bound state can exist in the $\bar{K}\bar{K}N$ system too. The three $\bar{K}N$ potentials were used, and a quasi-bound state was found with smaller binding energy than in the K^-pp and larger width. It is interesting, that the parameters of the state allow to associate it with a Ξ state mentioned in the Particle Data Group [28].

The paper summarises results of the series of exact or accurate calculations [3; 4; 14; 17; 21; 23; 24; 25; 27]. The next section contains information about the two-body interactions, necessary for the three-body calculations. Faddeev-type Alt-Grassberger-Sandhas equations with coupled channels, which were used for three-body calculations with strong interactions, are described in Section 3. Section 4 is devoted to the quasi-bound states in the K^-pp, K^-d, and K^-K^-p systems. The near-threshold K^-d scattering is considered in Section 5, the kaonic deuterium – in Section 6. The last section summarises the results.

2 Two-body interactions

In order to investigate some three-body system it is necessary to know the interactions of all the pairs of the particles. The interactions, necessary for investigations of the $\bar{K}NN - \pi\Sigma N$ and $\bar{K}\bar{K}N - \bar{K}\pi\Sigma$ systems, are $\bar{K}N$ and ΣN with other channels coupled to them, and the one-channel NN and $\bar{K}\bar{K}$ interactions (the rest of them were omitted in the three-body calculations). All potentials, except one of the NN potentials, were specially constructed for the calculations. They have a separable form and $\mathbb{N}$-term structure

$$V^{\alpha\beta}_{i,II'} = \sum_{m=1}^{\mathbb{N}^\alpha_i} \lambda^{\alpha\beta}_{i(m),II'} \, |g^{\alpha}_{i(m),I}\rangle\langle g^{\beta}_{i(m),I'}|, \tag{1}$$

which leads to a separable T-matrix

$$T^{\alpha\beta}_{i,II'} = \sum_{m,n=1}^{\mathbb{N}^\alpha_i} |g^{\alpha}_{i(m),I}\rangle \tau^{\alpha\beta}_{i(mn),II'} \langle g^{\beta}_{i(n),I'}| \,. \tag{2}$$

$\mathbb{N}^\alpha_i$ in Eq. (1) and Eq. (2) is a number of terms of the separable potential, λ is a strength constant, while g is a form-factor. The two-body isospin I in general is not conserved. In particular, the two-body isospin is conserved in the phenomenological $\bar{K}N - \pi\Sigma$ potentials, but not in the corresponding

T-matrices due to Coulomb interaction and the physical masses, taken into account. The chirally motivated $\bar{K}N-\pi\Sigma-\pi\Lambda$ potential does not conserve the isospin due to its energy and mass dependence.

The separable potentials are simpler than other models of interactions. However, the potentials, entering the equations for the antikaon-nucleon systems, were constructed in such a way that they reproduce the low-energy experimental data for every subsystem very accurately. From this point of view they are not worse than other models of the antikaon-nucleon or the Σ-nucleon interaction (in fact, they are even better than some chiral models). The one-term NN potential does not have a repulsive part, but the two-term model is repulsive at short distances. Finally, all three-body observables described in the present paper turned out to be dependent on the NN and ΣN interactions very weakly, therefore the most important is the accuracy of the $\bar{K}N$ potential.

The antikaon-nucleon interaction is the most important one for the three-body systems under consideration. There are several models of the $\bar{K}N$ interaction, some of them are "stand-alone" ones having the only aim to reproduce experimental data, others were used in few- of many-body calculations. The problem is that the first ones are too complicated to be used in few-body calculations, while the models from the second group are too simple to reproduce all the experimental data properly. Due to this, the $\bar{K}N$ potentials, which are simple enough for using in Faddeev-type three-body equations and at the same time reproduce all low-energy antikaon-nucleon experimental data, were constructed.

2.1 Antikaon-nucleon interaction, experimental data

$\Lambda(1405)$ resonance

The $\Lambda(1405)$ resonance is a manifestation of the attractive nature of the antikaon-nucleon interaction in isospin zero state, it couples $\bar{K}N$ to the lower $\pi\Sigma$ channel. Not only position and width, but the nature of the resonance itself are opened questions. A usual assumption is that $\Lambda(1405)$ is a resonance in the $\pi\Sigma$ channel and a quasi-bound state in the $\bar{K}N$ channel. According to the most recent Particle Data Group issue [28], the resonance has mass $1405.1^{+1.3}_{-1.0}$ MeV and width 50.5 ± 2.0 MeV. There is also an assumption suggested in [16] and supported by other chiral models, that the bump, which is usually understood as the $\Lambda(1405)$ resonance, is an effect of two poles. Due to this, the two different phenomenological models of the antikaon-nucleon interaction with one- or two-pole structure of the $\Lambda(1405)$ were constructed. The third model is a chirally motivated potential, which has two poles by construction.

Extraction of the resonance parameters from experimental data is complicated for two reasons. First, it cannot be studied in a two-body reaction and can be seen in a final state of some few- or many-body process. Second, its width is large, so the corresponding peak could be blurred.

A theoretical paper [22] was devoted to the possibility of tracing the $\Lambda(1405)$ resonance in the neutron spectrum of a K^-d breakup reaction. The neutron spectra of the $K^-d \to \pi\Sigma n$ reaction were calculated in center of mass energy range $0 - 50$ MeV. The three-body system with coupled $\bar{K}NN$ and $\pi\Sigma N$ channels was studied using the Faddeev-type AGS equations, described in Section 3, with four phenomenological $\bar{K}N$ potentials with one- or two-pole structure of $\Lambda(1405)$. It was found that kinematic effects completely mask the peak corresponding to the $\Lambda(1405)$ resonance. Therefore, comparison of eventual experimental data on the low-energy $K^-d \to \pi\Sigma n$ reaction with theoretical results hardly can give an answer to the question of the number of $\Lambda(1405)$ poles.

Later, similar calculations of the same process were performed for initial kaon momentum 1 GeV in [29; 30]. Coupled-channel AGS equations were solved as well with energy-dependent and -independent $\bar{K}N$ potentials. The authors predict a pronounced maximum in the double-differential cross section with a forward emitted neutron at $\pi\Sigma$ invariant mass 1.45 GeV. However, applicability of the $\bar{K}N$ potentials, fitted to the near-threshold data, and of the nonrelativistic Faddeev equations for such high energies is quite doubtful.

Several arguments, suggested in support to the idea of the two-pole structure of the $\Lambda(1405)$ resonance, were checked in [17] using the one- and two-pole phenomenological models of the antikaon-nucleon interaction. One of the arguments is the difference between the $\pi\Sigma$ cross-sections with different charge combinations, which is seen in experiments, e.g. in CLAS [31]. The elastic $\pi^+\Sigma^-$, $\pi^-\Sigma^+$, and $\pi^0\Sigma^0$ cross-sections were plotted to check the assumption, that the difference is caused by the two-pole structure. However, it turned out that the cross sections are different and their maxima are shifted one from each other for both one- and two-pole versions of the $\bar{K}N$ potential (see Fig. 5 of [17]). Therefore,

the effect is not a proof of the two-pole structure, but a manifestation of the isospin non-conservation and differences in the background.

Another argument for the two-pole structure comes from the fact, that the poles in a two-pole model are coupled to different channels. Indeed, a gradual switching off of the coupling between the $\bar{K}N$ and $\pi\Sigma$ channels turns the upper pole into a real bound state in $\bar{K}N$, while the lower one becomes a resonance in the uncoupled $\pi\Sigma$ channel (see e.g. Fig.2 of [23]). Consequently, it was suggested, that the poles of a two-body model manifest themselves in different reactions. In particular, the $\bar{K}N-\bar{K}N$, $\bar{K}N-\pi\Sigma$, and $\pi\Sigma-\pi\Sigma$ amplitudes should "feel" only one of the two poles. The hypothesis was also checked in [17], and indeed, the real parts of the $\bar{K}N-\bar{K}N$, $\bar{K}N-\pi\Sigma$, and $\pi\Sigma-\pi\Sigma$ amplitudes in $I=0$ state cross the real axis at different energies. But it is true for the both: the one- and the two-pole versions of the potential (see Fig. 6 of [17]). This effect must be caused by different background contributions in the reactions. Therefore, a proof of the two-pole structure of the $\bar{K}N$ interaction does not exist.

Cross-sections and threshold branching ratios

Three threshold branching ratios of the K^-p scattering

$$\gamma = \frac{\Gamma(K^-p\to\pi^+\Sigma^-)}{\Gamma(K^-p\to\pi^-\Sigma^+)} = 2.36\pm0.04, \tag{3}$$

$$R_c = \frac{\Gamma(K^-p\to\pi^+\Sigma^-,\pi^-\Sigma^+)}{\Gamma(K^-p\to\text{all inelastic channels})} = 0.664\pm0.011, \tag{4}$$

$$R_n = \frac{\Gamma(K^-p\to\pi^0\Lambda)}{\Gamma(K^-p\to\text{neutral states})} = 0.189\pm0.015 \tag{5}$$

were measured rather accurately in [32; 33]. Since the phenomenological $\bar{K}N$ potentials, used in the calculations, take the lowest $\pi\Lambda$ channel into account indirectly, a new ratio

$$R_{\pi\Sigma} = \frac{\Gamma(K^-p\to\pi^+\Sigma^-)+\Gamma(K^-p\to\pi^-\Sigma^+)}{\Gamma(K^-p\to\pi^+\Sigma^-)+\Gamma(K^-p\to\pi^-\Sigma^+)+\Gamma(K^-p\to\pi^0\Sigma^0)}\,, \tag{6}$$

which contains the measured R_c and R_n and has an "experimental" value

$$R_{\pi\Sigma} = \frac{R_c}{1-R_n\,(1-R_c)} \;=\; 0.709\pm0.011 \tag{7}$$

was constructed and used.

In contrast to the branching ratios, the elastic and inelastic total cross sections with K^-p in the initial state [35; 36; 37; 38; 39; 40] were measured not so accurately, see Figure 1.

Kaonic hydrogen

The most promising source of knowledge about the $\bar{K}N$ interaction is kaonic hydrogen atom (which correctly should be called "antikaonic hydrogen"). The atom has rich experimental history, several experiments measured its $1s$ level shift

$$\Delta E_{1s} = E_{1s}^{Coul} - \mathrm{Re}(E_{1s}^{Coul+Strong}) \tag{8}$$

and width Γ_{1s}, caused by the strong $\bar{K}N$ interaction in comparison to pure Coulomb case, with quite different results. The most recent measurement was performed by SIDDHARTA collaboration [18], their results are:

$$\Delta E_{1s}^{\mathrm{SIDD}} = -283\pm36\pm6\text{ eV},\quad \Gamma_{1s}^{\mathrm{SIDD}} = 541\pm89\pm22\text{ eV}. \tag{9}$$

Paradoxically, the directly measurable observables are not reproduced in the same way in the most of the theoretical works devoted to the antikaon-nucleon interaction. Some approximate formula are usually used for reproducing the $1s$ level shift. The most popular is a "corrected Deser" formula [34], which connects the shift with the scattering length a_{K^-p} of the K^-p system:

$$\Delta E^{cD} - i\,\frac{\Gamma^{cD}}{2} = -2\alpha^3\mu_{K^-d}^2\,a_{K^-p} \times[1-2\alpha\mu_{K^-p}\,a_{K^-p}\,(\ln\alpha-1)]. \tag{10}$$

Table 1 Physical characteristics of the three antikaon nucleon potentials: phenomenological $V^{1,SIDD}_{\bar{K}N-\pi\Sigma}$ and $V^{2,SIDD}_{\bar{K}N-\pi\Sigma}$ with one- and two-pole structure of the $\Lambda(1405)$ resonance respectively, and the chirally motivated $V^{Chiral}_{\bar{K}N-\pi\Sigma-\pi\Lambda}$ potential: $1s$ level shift $\Delta E^{K^-p}_{1s}$ (eV) and width $\Gamma^{K^-p}_{1s}$ (eV) of kaonic hydrogen, threshold branching ratios γ, R_c and R_n together with the experimental data. The additional $R_{\pi\Sigma}$ ratio, see Eq.(6), with its "experimental" value is shown as well. Scattering length of the K^-p system a_{K^-p} (fm) and pole(s) z_1, z_2 (MeV) forming the $\Lambda(1405)$ resonance are also demonstrated.

	$V^{1,SIDD}_{\bar{K}N-\pi\Sigma}$	$V^{2,SIDD}_{\bar{K}N-\pi\Sigma}$	$V^{Chiral}_{\bar{K}N-\pi\Sigma-\pi\Lambda}$	Experiment
$\Delta E^{K^-p}_{1s}$	-313	-308	-313	$-283 \pm 36 \pm 6$ [18]
$\Gamma^{K^-p}_{1s}$	597	602	561	$541 \pm 89 \pm 22$ [18]
γ	2.36	2.36	2.35	2.36 ± 0.04 [32; 33]
R_c	-	-	0.663	0.664 ± 0.011 [32; 33]
R_n	-	-	0.191	0.189 ± 0.015 [32; 33]
$R_{\pi\Sigma}$	0.709	0.709	-	0.709 ± 0.011 Eq.(7)
a_{K^-p}	-0.76 + i 0.89	-0.74 + i 0.90	-0.77 + i 0.84	
z_1	1426 - i 48	1414 - i 58	1417 - i 33	
z_2	-	1386 - i 104	1406 - i 89	

The formula is one of quite a few versions of the original formula, derived by Deser for the pion-nucleon system. It differs from the original one by the second term in the brackets. However, it was shown (e.g. in [14] and other papers) that for the antikaon-nucleon system the formula is not accurate, it gives $\sim 10\%$ error.

2.2 Phenomenological and chirally motivated $\bar{K}N$ potentials

The constructed phenomenological models of antikaon-nucleon interaction with one- or two-pole structure of the $\Lambda(1405)$ resonance together with the chirally motivated model reproduce the $1s$ level shift and width of kaonic hydrogen, measured by SIDDHARTA collaboration, directly, without using approximate formulas. The potentials also reproduce the experimental data on the K^-p scattering and the threshold branching ratios, described in the previous subsection. All three potentials are suitable for using in accurate few-body equations.

The problem of two particles interacting by the strong and Coulomb potentials, considered on the equal basis, was solved. The method of solution of Lippmann-Schwinger equation for a system with Coulomb plus a separable strong potential is based on the fact that the full T-matrix of the problem can be written as a sum $T = T^c + T^{sc}$. Here T_c is the pure Coulomb transition matrix and T^{sc} is the Coulomb-modified strong T-matrix. It was necessary to extend the formalism to describe the system of the coupled $\bar{K}N$, $\pi\Sigma$ (and $\pi\Lambda$ for the chirally motivated potential) channels. The physical masses of the particles were used in the equation, therefore, the two-body isospin of the system is not conserved. More details on the formalism can be found in [14].

The phenomenological potentials describing the $\bar{K}N$ system with coupled $\pi\Sigma$ channel are the one-term separable ones defined by Eq.(1). In momentum representation they have a form

$$V_I^{\bar{\alpha}\bar{\beta}}(k^{\bar{\alpha}}, k'^{\bar{\beta}}) = \lambda_I^{\bar{\alpha}\bar{\beta}}\, g^{\bar{\alpha}}(k^{\bar{\alpha}})\, g^{\bar{\beta}}(k'^{\bar{\beta}}), \tag{11}$$

where indices $\bar{\alpha}, \bar{\beta} = 1, 2$ denote the $\bar{K}N$ or $\pi\Sigma$ channel respectively, and I is a two-body isospin. Different form-factors were used for the one- and two-pole versions of the phenomenological potential. While for the one-pole version Yamaguchi form-factors

$$g^{\bar{\alpha}}(k^{\bar{\alpha}}) = \frac{1}{(k^{\bar{\alpha}})^2 + (\beta^{\bar{\alpha}})^2} \tag{12}$$

were used, the two-pole version has slightly more complicated form-factors in the $\pi\Sigma$ channel

$$g^{\bar{\alpha}}(k^{\bar{\alpha}}) = \frac{1}{(k^{\bar{\alpha}})^2 + (\beta^{\bar{\alpha}})^2} \; + \; \frac{s\,(\beta^{\bar{\alpha}})^2}{[(k^{\bar{\alpha}})^2 + (\beta^{\bar{\alpha}})^2]^2}\,. \tag{13}$$

In the $\bar{K}N$ channel the form-factor of the two-pole version is also of Yamaguchi form Eq.(12).

Range parameters $\beta^{\bar{\alpha}}$, strength parameters $\lambda_I^{\bar{\alpha}\bar{\beta}}$ and an additional parameter s of the two-pole version were obtained by fitting to the experimental data described in the previous subsection. They are: the elastic and inelastic K^-p cross-sections, the threshold branching ratios and the $1s$ level shift and width of kaonic hydrogen. The first versions of the potentials, presented in [14] and used in [17], were fitted to the KEK data [20] on kaonic hydrogen. The actual versions of the phenomenological potentials were fitted to the most recent experimental data of SIDDHARTA collaboration [18]. The parameters of the one- and two-pole versions of the phenomenological potentials fitted to SIDDHARTA data can be found in [21].

All fits were performed directly to the experimental values except the threshold branching ratios R_c and R_n. The reason is that the ratios contain data on scattering of K^-p into all inelastic channels including $\pi\Lambda$, which is taken by the phenomenological potentials into account only indirectly through imaginary part of one of the λ parameters. Due to this the phenomenological potentials were fitted to the new ratio $R_{\pi\Sigma}$, defined in Eq.(7).

The third model of the antikaon-nucleon interaction is the chirally motivated potential. It connects all three open channels: $\bar{K}N$, $\pi\Sigma$ and $\pi\Lambda$, and has a form

$$V_{II'}^{\alpha\beta}(k^\alpha, k'^\beta; \sqrt{s}) = g_I^\alpha(k^\alpha)\, \bar{V}_{II'}^{\alpha\beta}(\sqrt{s})\, g_{I'}^\beta(k'^\beta)\,, \tag{14}$$

where $V_{II'}^{\alpha\beta}(\sqrt{s})$ is the energy dependent part of the potential in isospin basis. In particle basis the energy dependent part has a form

$$\bar{V}^{ab}(\sqrt{s}) = \sqrt{\frac{M_a}{2\omega_a E_a}}\, \frac{C^{ab}(\sqrt{s})}{(2\pi)^3 f_a f_b}\, \sqrt{\frac{M_b}{2\omega_b E_b}}\,. \tag{15}$$

Indices a, b here denote the particle channels $a, b = K^-p, \bar{K}^0n, \pi^+\Sigma^-, \pi^0\Sigma^0, \pi^-\Sigma^+$ and $\pi^0\Lambda$. the square roots with baryon mass M_a, baryon energy E_a and meson energy w_a of the channel a ensure proper normalization of the corresponding amplitude. SU(3) Clebsh-Gordan coefficients C_I^{WT} enter the non-relativistic form of the leading order Weinberg-Tomozawa interaction

$$C^{ab}(\sqrt{s}) = -C^{WT}\,(2\sqrt{s} - M_a - M_b). \tag{16}$$

Since, as in the case of the phenomenological potentials, the physical masses of the particles were used, the two-body isospin I in Eq.(14) is not conserved. It is different from the phenomenological potentials situation since in that case the potentials conserve the two-body isospin (but the corresponding T-matrices do not). Another feature, which distinguish the chirally motivated potential from the phenomenological ones, is the isospin dependence of its form-factors:

$$g_I^\alpha(k^\alpha) = \frac{(\beta_I^\alpha)^2}{(k^\alpha)^2 + (\beta_I^\alpha)^2}. \tag{17}$$

Besides, they are dimensionless due to the additional factor $(\beta_I^\alpha)^2$ in the numerator.

The pseudo-scalar meson decay constants f_π, f_K and the isospin dependent range parameters β_I^α are free parameters of the chirally motivated potential. They also were found by fitting the potential to the experimental data in the same way as in the phenomenological potentials case. The chirally-motivated $\bar{K}N - \pi\Sigma - \pi\Lambda$ potential reproduces the elastic and inelastic K^-p cross-sections, SIDDHARTA $1s$ level shift and width of kaonic hydrogen. In contrast to the phenomenological potentials, the chirally-motivated one directly reproduces all three K^-p branching ratios: γ, R_c and R_n. The parameters of the potential can be found in [23].

The $\Lambda(1405)$ resonance can manifest itself as a bump in elastic $\pi\Sigma$ cross-sections or in K^-p amplitudes. In the last case, the real part of the amplitude crosses zero, while the imaginary part has a maximum near the resonance position. It is demonstrated in [21] and [23] that the elastic $\pi\Sigma$ cross-sections, provided by the three potentials, have a bump near the PDG value [28] for the mass of the $\Lambda(1405)$ resonance with appropriate width.

The physical characteristics of the three antikaon-nucleon potentials are shown in Table 1. In addition, the K^-p scattering length a_{K^-p} and the pole(s) forming the $\Lambda(1405)$ resonance, given by the potentials, are demonstrated. The elastic and inelastic K^-p cross-sections, provided by the three potentials, are plotted in Figure 1 together with the experimental data. It is seen form the Table 1 and

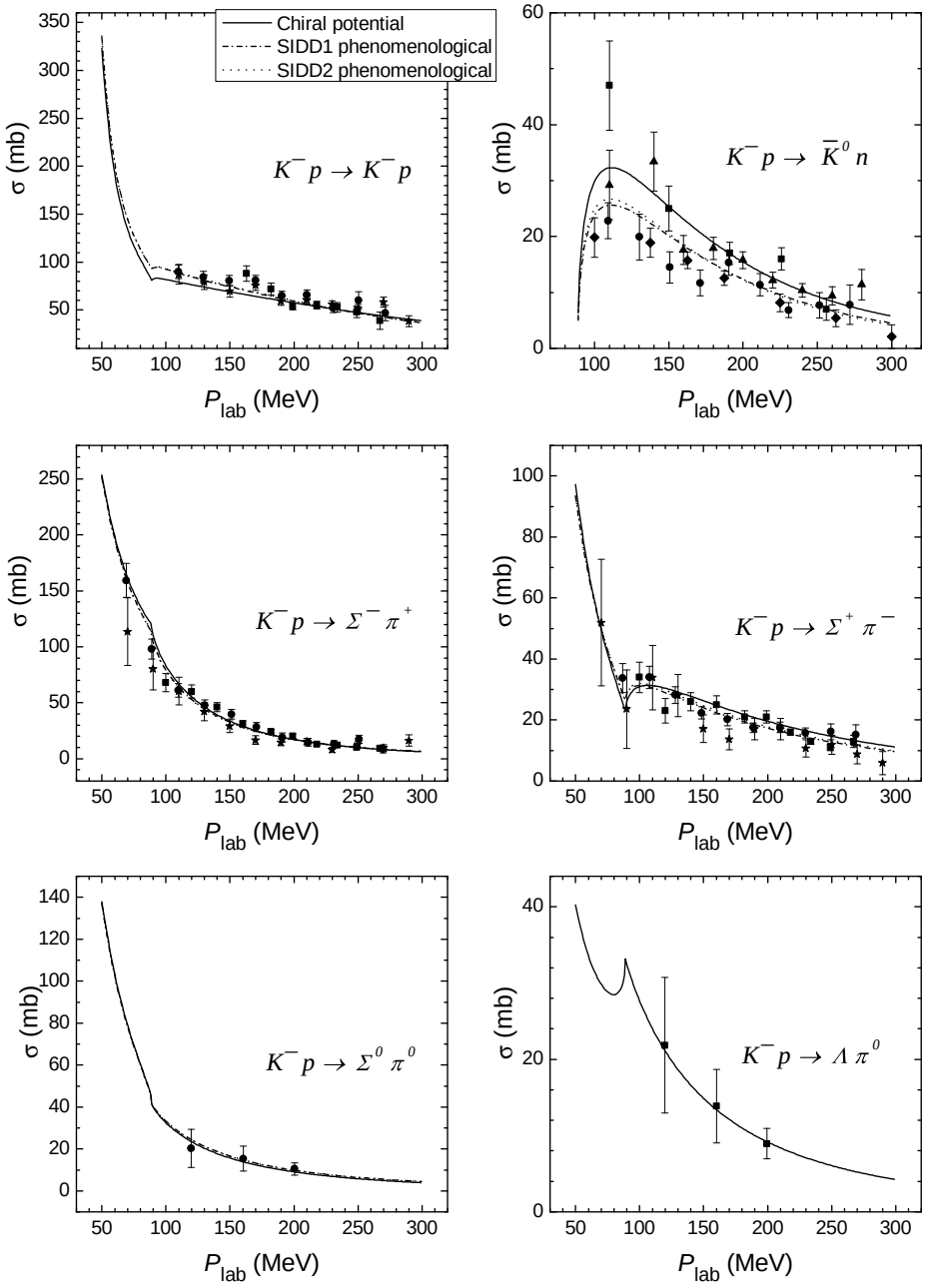

Fig. 1 Elastic and inelastic $K^- p$ cross-sections, obtained with the one-pole $V^{1,\mathrm{SIDD}}_{\bar{K}N-\pi\Sigma}$ (dash-dotted line), the two-pole $V^{2,\mathrm{SIDD}}_{\bar{K}N-\pi\Sigma}$ (dotted line) phenomenological potentials, and the chirally motivated $V^{Chiral}_{\bar{K}N-\pi\Sigma-\pi\Lambda}$ (solid line) potential. The experimental data are taken from [35; 36; 37; 38; 39; 40].

Figure 1 that the one- and two-pole phenomenological potentials and the chirally motivated potential describe the all experimental data with equal high accuracy. Therefore, it is not possible to choose one of the three models of the $\bar{K}N$ interaction looking at the two-body system.

Approximate versions of the coupled-channel potential

In order to check approximations used in other theoretical works, two approximate versions of the coupled-channel potentials Eq.(11), which have only one $\bar{K}N$ channel, were also used. They are: an exact optical potential and a simple complex one.

The exact optical one-channel potential, corresponding to a two-channel one, is given by Eq. (11) with $\bar{\alpha}, \bar{\beta} = 1$ and the strength parameter defined as

$$\lambda_I^{11,\mathrm{Opt}} = \lambda_I^{11} + \frac{(\lambda_I^{12})^2 \, \langle g_I^2 | \, G_0^{(2)}(z^{(2)}) | \, g_I^2 \rangle}{1 - \lambda_I^{22} \, \langle g_I^2 | \, G_0^{(2)}(z^{(2)}) | \, g_I^2 \rangle} \, . \tag{18}$$

Here $\lambda_I^{\bar{\alpha},\bar{\beta}}$ are the strength parameters of the two-channel potential, and $|g_I^2\rangle$ is the form-factor of the second channel. Since a two-body free Green's function $G_0^{(2)}$ depends on the corresponding two-body energy, the parameter $\lambda_I^{11,\mathrm{Opt}}$ of the exact optical potential is an energy-dependent complex function. The exact optical potential has exactly the same elastic amplitudes of the $\bar{K}N$ scattering as the elastic part of the full potential with coupled channels.

A simple complex potential is quite often miscalled "an optical" one, however, it is principally different. The strength parameter $\lambda_I^{11,\mathrm{Complex}}$ of a simple complex potential is a complex constant, therefore, the simple complex potential is energy independent. The strength parameter of a simple complex potential is usually chosen in such a way, that the potential reproduces only some characteristics of the interaction. The simple complex potential as well as the exact optical one take into account flux losses into inelastic channels through imaginary parts of the strength parameters.

2.3 Nucleon-nucleon and $\Sigma N(-\Lambda N)$ potentials

NN interaction

Different NN potentials, in particular, TSA-A, TSA-B and PEST, were used in order to investigate dependence of the three-body results on the nucleon-nucleon interaction models.

A two-term separable NN potential [41], called TSA, reproduces Argonne $V18$ [42] phase shifts and, therefore, is repulsive at short distances. Two versions of the potential (TSA-A and TSA-B) with slightly different form-factors

$$g_{(m)}^{A,NN}(k) = \sum_{n=1}^{2} \frac{\gamma_{(m)n}^{A}}{(\beta_{(m)n}^{A})^2 + k^2}, \quad \text{for } (m) = 1, 2 \tag{19}$$

$$g_{(1)}^{B,NN}(k) = \sum_{n=1}^{3} \frac{\gamma_{(1)n}^{B}}{(\beta_{(1)n}^{B})^2 + k^2}, \quad g_{(2)}^{B,NN}(k) = \sum_{n=1}^{2} \frac{\gamma_{(2)n}^{B}}{(\beta_{(2)n}^{B})^2 + k^2}$$

were used. TSA-A and TSA-B potentials properly reproduce the NN scattering lengths and effective radii, they also give correct binding energy of the deuteron in the $^3S_1$ state. For more details see Ref. [17].

A separabelization of the Paris model of the NN interaction, called PEST potential [43], was also used. The strength parameter of the one-term PEST is equal to -1, while the form-factor is defined by

$$g_I^{NN}(k) = \frac{1}{2\sqrt{\pi}} \sum_{n=1}^{6} \frac{c_{n,I}^{NN}}{k^2 + (\beta_{n,I}^{NN})^2} \tag{20}$$

with $c_{n,I}^{NN}$ and $\beta_{n,I}^{NN}$ being the parameters. PEST is equivalent to the Paris potential on and off energy shell up to $E_{\mathrm{lab}} \sim 50$ MeV. It also reproduces the deuteron binding energy in the $^3S_1$ state, as well as the triplet and singlet NN scattering lengths.

The quality of reproducing the $^3S_1$ phase shifts by the three NN potentials is shown in Fig.8 of [17], were they are compared with those given by the Argonne V18 model. The two-term TSA-A and

TSA-B potentials are very good at reproducing of the Argonne V18 phase shifts. They cross the real axis, which is a consequence of the NN repulsion at short distances. The one-term PEST potential does not have such a property, but its phase shifts are also close to the "standard" ones at lower energies.

Only isospin-singlet NN potential enters the AGS equations for the K^-d system and only isospin-triplet one enters the equations describing the K^-pp system after antisymmetrization.

ΣN interaction

A spin dependent $V^{\rm Sdep}$ and an independent of spin $V^{\rm Sind}$ versions of the ΣN potential were constructed in [17] in such a way, that they reproduce the experimental ΣN and ΛN cross-sections [44; 45; 46; 47; 48]. The one-term separable potentials with Yamaguchi form-factors were used for the two possible isospin states, but with different number of the channels.

Parameters of the one-channel $I = \frac{3}{2}$ state were fitted to the $\Sigma^+p \to \Sigma^+p$ cross-sections. The ΣN system in isospin one half state is connected to the ΛN channel, therefore, a coupled-channel potential of the $I = \frac{1}{2}$ $\Sigma N - \Lambda N$ interaction was constructed first. The coupled-channel $I = \frac{1}{2}$ potential together with the one-channel $I = \frac{3}{2}$ potential reproduce the $\Sigma^-p \to \Sigma^-p$, $\Sigma^-p \to \Sigma^0n$, $\Sigma^-p \to \Lambda n$, and $\Lambda p \to \Lambda p$ cross-sections. It is seen in Fig.9 of [17] that both $V^{\rm Sdep}$ and $V^{\rm Sind}$ versions of the $I = 3/2$ ΣN and $I = 1/2$ $\Sigma N - \Lambda N$ potentials reproduce the experimental data perfectly. Parameters of the potentials and the scattering lengths $a^{\Sigma N}_{\frac{1}{2}}$, $a^{\Sigma N}_{\frac{3}{2}}$, and $a^{\Lambda N}_{\frac{1}{2}}$, given by them, are shown in Table 5 of [17].

For the three-body $\bar{K}NN$ calculations, where a channel containing Λ is not included directly, not a coupled-channel, but one-channel ΣN models of the interaction in the $I = \frac{1}{2}$ state were used. They are an exact optical $V^{\Sigma N,{\rm Opt}}$ potential and a simple complex $V^{\Sigma N,{\rm Complex}}$ one, corresponding to the $I = \frac{1}{2}$ $\Sigma N - \Lambda N$ model with coupled channels. The exact optical potential has an energy dependent strength parameter defined by Eq. (18), it reproduces the elastic ΣN amplitude of the corresponding two-channel potential exactly. The simple complex potential gives the same scattering lengths, as the two-channel potential.

2.4 Antikaon-antikaon interaction

Lack of an experimental information on the $\bar{K}\bar{K}$ interaction means that it is not possible to construct the $\bar{K}\bar{K}$ potential in the same way as the $\bar{K}N$ or ΣN ones. Due to this, theoretical results of a modified model describing the $\pi\pi - K\bar{K}$ system developed by the Jülich group [49; 50] were used. The original model yields a good description of the $\pi\pi$ phase shifts up to partial waves with total angular momentum $J = 2$ and for energies up to $z_{\pi\pi} \approx 1.4$ GeV. In addition, the $f_0(980)$ and $a_0(980)$ mesons result as dynamically generated states.

Based on the underlying SU(3) flavor symmetry, the interaction in the $\bar{K}\bar{K}$ system was directly deduced from the $K\bar{K}$ interaction without any further assumptions. The $\bar{K}\bar{K}$ scattering length predicted by the modified Jülich model is $a_{\bar{K}\bar{K},I=1} = -0.186$ fm, therefore, it is a repulsive interaction. This version of the $\bar{K}\bar{K}$ interaction was called "Original".

Recent results for the KK scattering length from lattice QCD simulations suggest values of $a_{\bar{K}\bar{K},I=1} = (-0.141 \pm 0.006)$ fm [51] and $a_{\bar{K}\bar{K},I=1} = (-0.124 \pm 0.006 \pm 0.013)$ fm [52]. Those absolute values are noticeably smaller than the one predicted by the Original Jülich meson-exchange model and, accordingly, imply a somewhat less repulsive $\bar{K}\bar{K}$ interaction. Due to this, another version of the interaction that is in line with the lattice QCD results was also constructed. It yields scattering length $a_{\bar{K}\bar{K},I=1} = -0.142$ fm. This version of the $\bar{K}\bar{K}$ interaction was called "Lattice motivated".

However, the models of the $\bar{K}\bar{K}$ interaction described above cannot be directly used in the AGS equations. Due to this, the $\bar{K}\bar{K}$ interaction was represented in a form of the one-term separable potential with form factors given by

$$g(k) = \frac{1}{\beta_1^2 + k^2} + \frac{\gamma}{\beta_2^2 + k^2}. \qquad (21)$$

The strength parameters λ, γ and range parameters β were fixed by fits to the $\bar{K}\bar{K}$ phase shifts and scattering lengths of the "Original" and the ''Lattice motivated" models of the antikaon-antikaon interaction.

3 AGS equations for coupled $\bar{K}NN - \pi\Sigma N$ and $\bar{K}\bar{K}N - \bar{K}\pi\Sigma$ channels

The three-body Faddeev equations in the Alt-Grassberger-Sandhas (AGS) form [53] were used for the most of the three-body calculations. The equations were extended in order to take the $\pi\Sigma$ channel, coupled to the $\bar{K}N$ subsystem, directly. In practice it means that all operators entering the system

$$U_{ij}^{\alpha\beta} = \delta_{\alpha\beta}\,(1-\delta_{ij})\;(G_0^{\alpha})^{-1} + \sum_{k,\gamma=1}^{3}(1-\delta_{ik})\,T_k^{\alpha\gamma}\,G_0^{\gamma}\,U_{kj}^{\gamma\beta}\,, \tag{22}$$

namely, transition operators U_{ij}, two-body T-matrices T_i and the free Green function G_0, - have additional channel indices $\alpha, \beta = 1, 2, 3$ in addition to the Faddeev partition indices $i, j = 1, 2, 3$. The additional $\pi\Sigma N$ ($\alpha = 2$) and $\pi N\Sigma$ ($\alpha = 3$) channels were added to the $\bar{K}NN$ system , while the $\bar{K}\bar{K}N$ system was extended to the $\bar{K}\pi\Sigma$ ($\alpha = 2$) and $\pi\bar{K}\Sigma$ ($\alpha = 3$) channels. A Faddeev index i, as usual, defines a particle and the remained pair, now in the particular particle channel α. The combinations of the (i, α) indices with possible two-body isospin values can be found in [4] for the $\bar{K}NN$ system and in [27] for the $\bar{K}\bar{K}N$ systems, respectively.

Since the separable potentials Eq.(1), leading to the separable T-matrices Eq.(2), were used as an input, the system Eq.(22) turned into the new system of operator equations

$$X_{ij,I_iI_j}^{\alpha\beta} = \delta_{\alpha\beta}\,Z_{ij,I_iI_j}^{\alpha} + \sum_{k=1}^{3}\sum_{\gamma=1}^{3}\sum_{I_k} Z_{ik,I_iI_k}^{\alpha}\,\tau_{k,I_k}^{\alpha\gamma}\,X_{kj,I_kI_j}^{\gamma\beta} \tag{23}$$

with $X_{ij,I_iI_j}^{\alpha\beta}$ and $Z_{ij,I_iI_j}^{\alpha\beta}$ being new transition and kernel operators respectively

$$X_{ij,I_iI_j}^{\alpha\beta} = \langle g_{i,I_i}^{\alpha}|G_0^{\alpha}\,U_{ij,I_iI_j}^{\alpha\beta}G_0^{\beta}|g_{j,I_j}^{\beta}\rangle\,, \tag{24}$$

$$Z_{ij,I_iI_j}^{\alpha\beta} = \delta_{\alpha\beta}\,Z_{ij,I_iI_j}^{\alpha} = \delta_{\alpha\beta}\,(1-\delta_{ij})\,\langle g_{i,I_i}^{\alpha}|G_0^{\alpha}|g_{j,I_j}^{\alpha}\rangle\,. \tag{25}$$

$\underline{\bar{K}NN - \pi\Sigma N \text{ system}}$

The two states of the strangeness $S = -1$ $\bar{K}NN$ system were considered. The K^-pp and K^-d systems differ from each another by the total spin value, which leads to different symmetry of the operators describing the system containing two identical baryons, NN. This fact is taken into account when the three-body coupled-channel equations are antisymmetrized.

All calculations were performed under or slightly above the $\bar{K}NN$ threshold, so that orbital angular momentum of all two-body interactions was set to zero and, therefore, the total orbital angular momentum is also $L = 0$. In particular, the main $\bar{K}N$ potential was constructed with orbital angular momentum $l = 0$ since the interaction is dominated by the s-wave $\Lambda(1405)$ resonance. The interaction of π-meson with a nucleon is weaker than the other interactions, therefore, it was omitted in the equations. An experimental information about the ΣN interaction is very poor, and there is no reason to assume significant effect of higher partial waves. Finally, the NN interaction was also taken in $l = 0$ state only, since physical reasons for sufficient effect of higher partial waves in the present calculation are not seen.

Spin of the $\bar{K}NN$ system is given by spin of the two baryons, which also defines the NN isospin due to the symmetry properties. Looking for the quasi-bound state in $\bar{K}NN$, the isospin $I = 1/2$ and spin zero state, usually denoted as K^-pp, was chosen due to its connection to experiment. Another possible configuration with the same isospin and spin one, which is K^-d, was also studied. As for the $\bar{K}NN$ state with isospin $I = 3/2$, it is governed by the isospin $I_i = 1$ $\bar{K}N$ interaction, which is much weaker attractive than the one in the $I_i = 0$ state or even repulsive. Therefore, no quasi-bound state is expected there.

The nucleons, entering the highest $\bar{K}NN$ channel, require antisymmetrization of the operators entering the system of equations Eq.(23). Two identical baryons with symmetric spatial components ($L_i = 0$) has antisymmetric ($S_i = 0$) spin components for the pp state of the NN subsystem or symmetric ($S_i = 1$) ones for the d state. The operator $X_{1,1}^{1}$ has symmetric NN isospin components, therefore, it has the correct symmetry properties for the K^-pp system (here and in what follows the right-hand indices of X are omitted: $X_{ij,I_iI_j}^{\alpha\beta} \to X_{i,I_i}^{\alpha}$). Another operator, $X_{1,0}^{1}$, has antisymmetric NN

isospin components, so it drops out the equations for the K^-pp system, but remains in the equations describing the K^-d system. All the remaining operators form symmetric and antisymmetric pairs. At the end there is a system of 9 (with PEST NN potential) or 10 (with TSA nucleon-nucleon model) coupled operator equations, which has the required symmetry properties.

The system of operator equations Eq. (23) written in momentum space turns into a system of integral equations. To search for a quasi-bound state in a three-body system means to look for a solution of the homogeneous system corresponding to Eq. (23). Calculation of three-body scattering amplitudes require solution of the inhomogeneous system. In the both cases the integral equations are transformed into algebraic ones. The methods of solution are different for the quasi-bound state and scattering problems, so they are discussed in the corresponding sections.

More details on the three-body equations with coupled $\bar{K}NN - \pi\Sigma N$ channels can be found in [4] for the K^-pp and in [17] for the K^-d systems.

$\bar{K}\bar{K}N - \bar{K}\pi\Sigma$ system

As for the strangeness $S = -2$ $\bar{K}\bar{K}N$ system, its total spin is equal to one half since an antikaon is a pseudoscalar meson. Since the two-body interactions, namely the $\bar{K}N - \pi\Sigma$ and $\bar{K}\bar{K}$ potentials, were chosen to have zero orbital angular momentum, the total angular momentum is also equal to $1/2$. As in the case of the $\bar{K}NN$ system, the state of the $\bar{K}\bar{K}N$ system with the lowest possible value of the isospin $I = 1/2$ was considered.

Two identical antikaons should have a symmetric way function, therefore, the $\bar{K}\bar{K}$ pair in s-wave can be in isospin one state only. Accordingly, the three-body operators entering the AGS system for the $\bar{K}\bar{K}N$ system were symmetrized. Similarly to the $\bar{K}NN$ case, the transition operator $X^1_{3,1}$, entering the equations describing $\bar{K}\bar{K}N$, already has the proper symmetry properties. The remaining operators form pairs with proper symmetry properties.

It is necessary to note that while Coulomb potential was directly included in the two-body equations, used for fitting the antikaon-nucleon potentials, the three-body calculations were performed without it (except the case of kaonic deuterium calculations, of cause). The reason is that the expected effect of its inclusion is small. In addition, the isospin averaged masses were used in all three-body calculations in contrast to the two-body $\bar{K}N$ case. Accuracy of this approximation was checked in [22], and it turned out to be quite high.

4 Quasi-bound states

It was shown in Section 2.2 that the phenomenological $\bar{K}N$ potentials with one- and two-pole structure of the $\Lambda(1405)$ resonance and the chirally motivated antikaon-nucleon potential can reproduce near-threshold experimental data on K^-p scattering and kaonic hydrogen with equal accuracy. Therefore, it is not possible to choose one of these models looking at the two-body system only. Due to this, the three-body calculations were performed using all three models of the antikaon-nucleon interaction.

The quasi-bound state in the K^-pp system was the phenomenon, which attracted the present interest to the antikaon-nucleus systems. Additionally to being an interesting exotic object, the state could clarify still unanswered questions on the antikaon-nucleon interaction, in particular, the nature of the $\Lambda(1405)$ resonance.

$\bar{K}\bar{K}N$ is one more possible candidate for a strange three-body system with the quasi-bound state in it. However, the strangeness $S = -2$ system contains $\bar{K}\bar{K}$ interaction, which is repulsive. The question was, whether the repulsion is strong enough to overtake $\bar{K}N$ attraction and by this exclude the possibility of the quasi bound state formation.

4.1 Two ways of a quasi-bound state evaluation

The quasi-bound state, which is a bound state with a non-zero width, for the higher $\bar{K}NN$ (or $\bar{K}\bar{K}N$) channel, is at the same time a resonance for the lower $\pi\Sigma N$ ($\bar{K}\pi\Sigma$) channel. Therefore, the corresponding pole should be situated between the $\bar{K}NN$ ($\bar{K}\bar{K}N$) and $\pi\Sigma N$ ($\bar{K}\pi\Sigma$)) thresholds on the physical energy sheet of the higher channel and on an unphysical sheet of the lower channel. Two methods of searching of the complex pole position by solving the homogeneous system of equations were used.

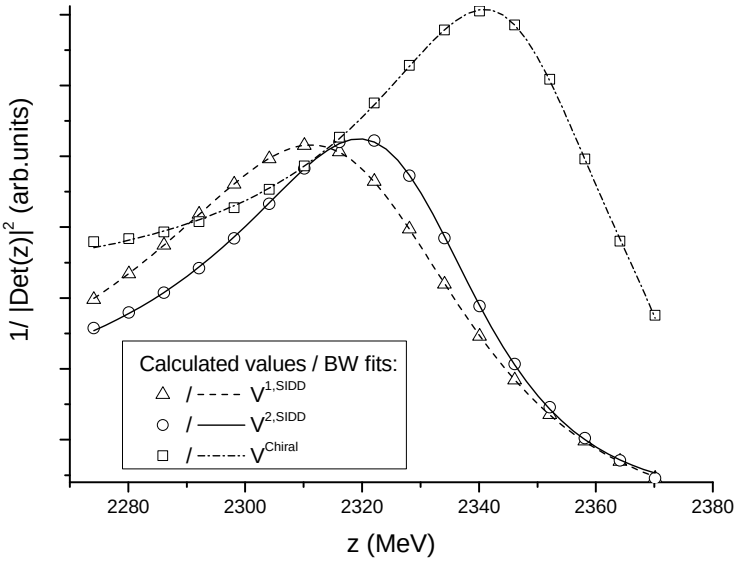

Fig. 2 Calculated $1/|\mathrm{Det}(z)|^2$ functions of the AGS system of equations for the K^-pp system (symbols) and the corresponding Breit-Wigner fits of the obtained curves (lines) [24] for the one-pole $V^{1,\mathrm{SIDD}}_{\bar{K}N-\pi\Sigma}$ (triangles and dashed line), the two-pole $V^{2,\mathrm{SIDD}}_{\bar{K}N-\pi\Sigma}$ (circles and solid line) phenomenological potentials, and the chirally motivated $V^{Chiral}_{\bar{K}N-\pi\Sigma-\pi\Lambda}$ (squares and dash-dotted line) potential.

.

The first one is the direct pole search with contour rotation. The correct analytical continuation of the equations from the physical energy sheet to the proper unphysical one is achieved by moving the momentum integration into the complex plane. Namely, the integration was performed along a ray in the fourth quadrant of the complex plane with some condition on the momentum variable. After that the position z_0 of a quasi-bound state was found by solving the equation $\mathrm{Det}(z_0) = 0$, where $\mathrm{Det}(z)$ is the determinant of the linear system, obtained after discretization of the integral equations, corresponding to Eq. (23).

Another way of a quasi-bound state searching, which avoids integration in the complex plane, was suggested and used in [24]. The idea is that every isolated and quite narrow resonance should manifest itself at real energies. Namely, resonances are usually seen in cross-sections of some reactions. The function $1/\mathrm{Det}(z)$ enters all possible amplitudes, described by a system of three-body integral equations. Therefore, the function $1/|\mathrm{Det}(z)|^2$, entering all possible cross-sections, can be calculated instead of some cross-sections. The function is universal, it does not contain additional information about the particular processes in the three-body system. The corresponding bump of the $1/|\mathrm{Det}(z)|^2$ function, calculated at real energies, can be fitted by a Breit-Wigner curve with arbitrary background. In this way an information on the resonance position and width can be obtained.

It is clear that the second method can work only if the resonance bump is isolated and not too wide. The bump corresponding to the K^-pp quasi-bound state satisfies these conditions [24], as is seen in Fig. 2. The calculated $1/|\mathrm{Det}(z)|^2$ functions of the AGS system of equations are shown there as symbols while the corresponding Breit-Wigner fitting curves are drown in lines. The results obtained with the three $\bar{K}N$ potentials, described in Section 2.2, are shown in the figure.

Since direct search of the complex root is a non-trivial task, the Breit-Wigner values of the $1/|\mathrm{Det}(z)|^2$ function can give a good starting point for it. On the other hand, the $1/|\mathrm{Det}(z)|^2$ method can be used as a test of the directly found pole position, which is free of the possible uncertainty of the proper choice of the Riemann sheet. However, the $1/|\mathrm{Det}(z)|^2$ method is not easier than the direct search, since the calculation of the determinant, which is almost equal to the solving of a scattering problem, should be performed.

Table 2 Binding energy B_{K^-pp} (MeV) and width Γ_{K^-pp} (MeV) of the quasi-bound state in the K^-pp system [24]: the results of the direct pole search and of the Breit-Wigner fit of the $1/|\mathrm{Det(z)}|^2$ function at real energy axis. The AGS calculations were performed with the one-pole $V^{1,SIDD}_{\bar{K}N-\pi\Sigma}$, two-pole $V^{2,SIDD}_{\bar{K}N-\pi\Sigma}$ phenomenological potentials from [21] and the chirally motivated $V^{Chiral}_{\bar{K}N-\pi\Sigma-\pi\Lambda}$ potential from [23].

	Direct pole search		BW fit of $1/\|\mathrm{Det(z)}\|^2$	
	B_{K^-pp}	Γ_{K^-pp}	B_{K^-pp}	Γ_{K^-pp}
$V^{1,SIDD}_{\bar{K}N-\pi\Sigma}$	53.3	64.8	54.0	66.6
$V^{2,SIDD}_{\bar{K}N-\pi\Sigma}$	47.4	49.8	46.2	51.8
$V^{\mathrm{Chiral}}_{\bar{K}N-\pi\Sigma-\pi\Lambda}$	32.2	48.6	30.3	46.6

4.2 K^-pp quasi-bound state: results

The first dynamically exact calculation of the quasi-bound state in the K^-pp system was published in [3], while the extended version of the results appeared in [4]. Existence of the $I = 1/2, J^\pi = 0^-$ three-body quasi-bound state in the $\bar{K}NN$ system, predicted in [1; 2], was confirmed there, but the evaluated binding energy and width were strongly different. However, the $\bar{K}N - \pi\Sigma$ potentials used in [3; 4] do not reproduce the experimental data on the K^-p system as accurately, as those described in Section 2.2. Due to this, the calculations devoted to the K^-pp system were repeated in [24]. The one-pole $V^{1,SIDD}_{\bar{K}N-\pi\Sigma}$, two-pole $V^{2,SIDD}_{\bar{K}N-\pi\Sigma}$ phenomenological potentials from [21] and the chirally motivated $V^{Chiral}_{\bar{K}N-\pi\Sigma-\pi\Lambda}$ potential from [23], described in Section 2.2, were used as an input. The other two potentials were the two-term TSA-B NN potential [41] together with the spin-independent exact optical ΣN potential in isospin $I = 1/2$ state and the one-channel $V_{\Sigma N}$ in $I = 3/2$, see Section 2.3.

The results of the last calculations [24] of the K^-pp quasi-bound state are shown in Table 2. First of all, comparison of the results obtained using the direct pole search and the $1/|\mathrm{Det}(z)|^2$ method demonstrates that they are very close each to other for the every given $\bar{K}N$ potential. Therefore, the suggested $1/|\mathrm{Det}(z)|^2$ method of finding mass and width of a subthreshold resonance is efficient for the K^-pp system, and the two methods supplement each another.

Another fact, seen from the results in Table 2, is strong dependence of the binding energy B_{K^-pp} of the quasi-bound state and its width Γ_{K^-pp} on the $\bar{K}N$ interaction models. It was already observed in [3; 4], when older phenomenological antikaon-nucleon potentials were used. In particular, it is seen from Table 2 that the quasi-bound states resulting from the phenomenological potentials lie about $15 - 20$ MeV deeper than those of the chirally motivated one. This probably is due to the energy dependence of the chirally motivated model of the interaction. Really, all three potentials were fitted to the experimental data near the $\bar{K}N$ threshold. When the K^-pp quasi-bound state is calculated at lower energies, the strengths of the phenomenological models of the $\bar{K}N$ interaction are unchanged. As for the chirally motivated potential, its energy dependence reduces the attraction at the lower energies in the $\bar{K}NN$ quasi-bound state region, thus producing the states with less binding.

The widths of the three quasi-bound states are also different: those of the two-pole models of the $\bar{K}N$ interaction are almost coinciding, while the width evaluated using the one-pole $V^{1,SIDD}_{\bar{K}N-\pi\Sigma}$ potential is much larger. It is seen from Table 1 that the potentials with the two-pole $\Lambda(1405)$ structure have very close positions of the higher poles, while the pole of the one-pole potential is different. Therefore, the difference in widths might be connected with the different pole structure of the corresponding $\bar{K}N$ interaction models.

Importance of the proper inclusion of the second $\pi\Sigma N$ channel in the calculations was first demonstrated in [4]. A simple complex version of the $\bar{K}N - \pi\Sigma$ potentials, described in Section 2.2, was used in [4] together with the full version with coupled channels. This allowed to check importance of the proper inclusion of the second channel. Comparison of the result of the one-channel complex calculation ($B^{1\,\mathrm{complex}}_{K^-pp}, \Gamma^{1\,\mathrm{complex}}_{K^-pp}$) with the coupled-channel one ($B^{2\,\mathrm{coupled}}_{K^-pp}, \Gamma^{2\,\mathrm{coupled}}_{K^-pp}$)

$$B^{2\,\mathrm{coupled}}_{K^-pp} = 55.1\ \mathrm{MeV} \qquad \Gamma^{2\,\mathrm{coupled}}_{K^-pp} = 101.8\ \mathrm{MeV} \tag{26}$$

$$B^{1\,\mathrm{complex}}_{K^-pp} = 40.2\ \mathrm{MeV} \qquad \Gamma^{1\,\mathrm{complex}}_{K^-pp} = 77.4\ \mathrm{MeV} \tag{27}$$

shows that the quasi-bound state obtained in the full calculation with coupled channels is much deeper and broader than the approximate one-channel one. (The values for the binding energy and width in Eq.(26) differ from those in Table 2 since another $\bar{K}N$ potential was used in [4].) This means that the $\pi\Sigma$ channel plays an important dynamical role in forming the three-body quasi-bound state, over its obvious role of absorbing flux from the $\bar{K}N$ channel. Thus, proper inclusion of the second $\pi\Sigma$ channel is crucial for the $\bar{K}NN$ system.

It was found later in [24] that use of the exact optical $\bar{K}N$ potential can serve an alternate way of direct inclusion of the $\pi\Sigma$ channel. An accuracy of use of the exact optical $\bar{K}N$ potential, which gives exactly the same on- and off-shell elastic $\bar{K}N$ amplitude as the original potential with coupled channels, was checked in one-channel AGS calculations for the three actual $\bar{K}N$ potentials. The "exact optical" binding energies differ only slightly from the full coupled-channel results from Table 2, while the widths gain more visible error:

$$B^{1,SIDD,Opt}_{K^-pp} = 54.2 \text{ MeV} \qquad \Gamma^{1,SIDD,Opt}_{K^-pp} = 61.0 \text{ MeV} \tag{28}$$

$$B^{2,SIDD,Opt}_{K^-pp} = 47.4 \text{ MeV} \qquad \Gamma^{2,SIDD,Opt}_{K^-pp} = 46.0 \text{ MeV} \tag{29}$$

$$B^{Chiral,Opt}_{K^-pp} = 32.9; \text{MeV} \qquad \Gamma^{Chiral,Opt}_{K^-pp} = 48.8 \text{ MeV}. \tag{30}$$

However, the difference in widths is not dramatic, so the one-channel Faddeev calculation with the exact optical $\bar{K}N$ potential could be quite satisfactory approximation to the full calculation with coupled channels.

4.3 K^-pp quasi-bound state: comparison to other results

The three binding energy B_{K^-pp} and width Γ_{K^-pp} values of the K^-pp quasi-bound state, shown in Table 2, can be compared with worth mentioning other theoretical results. Those are: the original prediction of the deep and narrow quasi-bound K^-pp state [1; 2], the results obtained in the earlier Faddeev calculation [4], the most recent results of alternative calculation using the same equations with different input [54] and two variational results [55; 56]. Only calculations presented in [54] together with the earlier ones [3; 4] were performed with directly included $\pi\Sigma N$ channel. All others take it into account approximately. The second problem is that none of the $\bar{K}N$ potentials, used in all other K^-pp calculations, reproduce data on near-threshold K^-p scattering with the same level of accuracy as those described in Section 2.2. In addition, none of them reproduce the $1s$ level shift of kaonic hydrogen directly.

The binding energy of the quasi-bound K^-pp state and its width were obtained in [1; 2] from a G-matrix calculation, which is a many-body technics. The one-channel simple complex $\bar{K}N$ potential used in those calculations does not reproduce the actual K^-p experimental data. Finally, the authors of [1; 2] take into account only the $\bar{K}NN$ channel. In a funny way all the defects of the calculation presented in [1; 2] led to the binding energy (48 MeV) and width (61 MeV), which are quite close to the exact results from Table 2 obtained with the two-pole and the one-pole phenomenological potentials, respectively.

The earlier result for the binding energy $B_{K^-pp} = 55.1$ MeV [4] is very close to the actual one from Table 2 calculated with the one-pole phenomenological $\bar{K}N - \pi\Sigma$ potential. In fact, in both cases the same three-body equations with coupled $\bar{K}NN$ and $\pi\Sigma N$ channels were solved. In addition, the same model of the antikaon-nucleon interaction was used, but with different sets of parameters. This difference influenced the width of the quasi-bound state: the older $\Gamma_{K^-pp} = 100.2$ MeV is much larger.

Coupled-channel AGS equations were also solved in [54] with chirally motivated energy dependent and independent $\bar{K}N$ potentials. Therefore, in principle, those results obtained with the energy dependent version of the $\bar{K}N$ potential $V^{E-dep}_{\bar{K}N}$ should give a result, which is close to those from Table 2 with chirally motivated model of interaction $V^{\text{Chiral}}_{\bar{K}N-\pi\Sigma-\pi\Lambda}$. However, only those width $(34 - 46$ MeV) is comparable to the $\Gamma^{\text{Chiral}}_{K^-pp}$, while the binding energy obtained in [54] $(9 - 16$ MeV) is much smaller than the actual one from Table 2. The situation is opposite when the actual results are compared with those obtained in [54] using the energy independent antikaon-nucleon potential. Namely, binding

energies reported in that paper ($44 - 58$ MeV) are comparable with those from Table 2 evaluated using phenomenological $V_{\bar{K}N}^{1,SIDD}$ and $V_{\bar{K}N}^{2,SIDD}$ potentials, however, their widths $34 - 40$ MeV are much smaller.

The authors of [54] neglect the ΣN interaction in their calculations. It was shown in [3; 4] that dependence of the three-body K^-pp pole position on ΣN is weak. However, when the interaction is switched off completely, like in the case of [54], some visible effect manifests itself.

An approximation used in the chirally motivated models used in [54] is more serious reason of the difference. Namely, the energy-dependent square root factors, responsible for the correct normalization of the $\bar{K}N$ amplitudes, are replaced by constant masses. This can be reasonable for the highest $\bar{K}N$ channel, however, it is certainly a poor approximation for the lower $\pi\Sigma$ and $\pi\Lambda$ channels. The role of this approximation in the AGS calculations was checked in [24], the obtained approximate binding energy 25 MeV is really much smaller than the original one 32 MeV, presented in Table 2. The remaining difference between the results from Table 2 and those from [54] could be explained by the lower accuracy of reproducing experimental K^-p data by the $\bar{K}N$ potentials from [54].

Finally, no second pole in the K^-pp system reported in [54] was found in [24]. The search was performed with all three $\bar{K}N$ potentials in the corresponding energy region (binding energy $67 - 89$ MeV and width $244 - 320$ MeV).

Variational calculations, performed by two groups, reported the results which are very close to those obtained in [54] with the energy-dependent potential: $B_{K^-pp} = 17 - 23$ MeV, $\Gamma_{K^-pp} = 40 - 70$ MeV in [55] and $B_{K^-pp} = 15.7$ MeV, $\Gamma_{K^-pp} = 41.2$ MeV in [56]. However, there are a few problematic points in [55; 56]. First of all, the variational calculations were performed solely in the $\bar{K}NN$ channel. The authors of the variational calculations used a one-channel $\bar{K}N$ potential, derived from a chirally motivated model of interaction with many couped channels. However, the potential is not the "exact optical" one. In fact, it is not clear, how this one-channel potential is connected to the original one and whether it still reproduces some experimental K^-p data.

Moreover, the position of the K^-pp quasi-bound state was determined in [55; 56] using only the real part of this complex $\bar{K}N$ potential, as a real bound state. The width was estimated as the expectation value of the imaginary part of the potential. This, essentially perturbative, treatment of the inelasticity might be justified for quite narrow resonances, but the K^-pp quasi-bound state is certainly not of this type.

Another serious problem of the variational calculations is their method of treatment of the energy dependence of the $\bar{K}N$ potential in the few-body calculations. It was already shown in the previous subsection that the energy dependence of the chirally motivated model of the $\bar{K}N$ interaction is very important for the K^-pp quasi-bound state position. While momentum space Faddeev integral equations allow the exact treatment of this energy dependence, variational calculations in coordinate space can use only energy independent interactions. Due to this the energy of the $\bar{K}N$ potential was fixed in [55; 56] at a "self-consistent" value $z_{\bar{K}N}$.

A series of calculations using the exact AGS equations was performed in [24] with differently fixed two-particle $\bar{K}N$ energies $z_{\bar{K}N}$ in the couplings of the chirally motivated interaction. The conclusion was, that it is not possible to define an "averaged" $z_{\bar{K}N}$, for which the fixed-energy chirally motivated interaction, even in the correct three-body calculation, can yield a correct K^-pp quasi-bound state position. First, the calculations of [24] show, that a real $z_{\bar{K}N}$ has absolutely no chance to reproduce or reasonably approximate the exact quasi-bound state position, even with correct treatment of the imaginary part of the interaction, unlike in [55; 56]. Second, the way, how the "self-consistent" value of (generally complex) $z_{\bar{K}N}$ is defined in the papers does not seem to guarantee, that the correct value will be reached or at least approximated. In view of the above considerations, the results of [55; 56] can be considered as rough estimates of what a really energy dependent $\bar{K}N$ interaction will produce in the K^-pp system.

After publication of the exact results [24] one more paper on the K^-pp system appeared [57]. Hyperspherical harmonics in the momentum representation and Faddeev equations in configuration space were used there. However, the authors collected all defects of other approximate calculations. In particular, they used simple complex antikaon-nucleon potentials and, therefore, neglected proper inclusion of the $\pi\Sigma N$ channel, which is crucial for the system. In addition, the $\bar{K}N$ potentials are those from [2; 55], which have problems with reproducing of the experimental K^-p data. Keeping all this in mind, the results of [57] hardly can be reliable.

Table 3 Binding energy $B_{\bar{K}\bar{K}N}$ (MeV) and width $\Gamma_{\bar{K}\bar{K}N}$ (MeV) of the quasi-bound state in the $\bar{K}\bar{K}N$ system [27]: the results of the direct pole search and of the Breit-Wigner fit of the $1/|\mathrm{Det(z)}|^2$ function at real energy axis. The AGS calculations were performed with the one-pole $V^{1,SIDD}_{\bar{K}N-\pi\Sigma}$, two-pole $V^{2,SIDD}_{\bar{K}N-\pi\Sigma}$ phenomenological potentials from [21] and the chirally motivated $V^{Chiral}_{\bar{K}N-\pi\Sigma-\pi\Lambda}$ potential from [23]. $V^{Orig}_{\bar{K}\bar{K}}$ and $V^{Lattice}_{\bar{K}\bar{K}}$ models of the antikaon-antikaon interaction were used.

		Direct pole search		BW fit of $1/\lvert\mathrm{Det(z)}\rvert^2$	
		$B_{\bar{K}\bar{K}N}$	$\Gamma_{\bar{K}\bar{K}N}$	$B_{\bar{K}\bar{K}N}$	$\Gamma_{\bar{K}\bar{K}N}$
$V^{Orig}_{\bar{K}\bar{K}}$ and	$V^{1,SIDD}_{\bar{K}N-\pi\Sigma}$	11.9	102.2	17.1	110.8
	$V^{2,SIDD}_{\bar{K}N-\pi\Sigma}$	23.1	91.4	23.7	77.6
	$V^{\mathrm{Chiral}}_{\bar{K}N-\pi\Sigma-\pi\Lambda}$	15.5	63.5	15.9	57.4
$V^{Lattice}_{\bar{K}\bar{K}}$ and	$V^{1,SIDD}_{\bar{K}N-\pi\Sigma}$	19.5	102.0	23.7	103.7
	$V^{2,SIDD}_{\bar{K}N-\pi\Sigma}$	25.9	84.6	26.4	76.8
	$V^{\mathrm{Chiral}}_{\bar{K}N-\pi\Sigma-\pi\Lambda}$	16.1	61.3	15.9	60.0

4.4 K^-d quasi-bound state

The strongly attractive isospin-zero part of the $\bar{K}N$ potential plays less important role in the spin-one K^-d state of the $\bar{K}NN$ system than in the spin-zero K^-pp. Therefore, if a quasi-bound state exists in K^-d, it should have smaller binding energy than in K^-pp. The Faddeev calculations of the K^-d scattering length a_{K^-d}, described in Section 5, gave some evidence that such a state could exists [23]. A simple analytical continuation of the effective range formula below the K^-d threshold suggests a K^-d quasi-bound state with binding energy $14.6 - 19.6$ MeV (the energy is measured from the K^-d threshold) and width $15.6 - 22.0$ MeV for the three antikaon-nucleon potentials from Section 2.2.

However, a systematic search for these states, performed in [23] with the same two-body input as for the K^-pp system, did not find the corresponding poles in the complex energy plane between the $\pi\Sigma N$ and K^-d thresholds. The reason of discrepancy between the effective range estimations and the direct calculations must be the validity of the effective range formula, which is limited to the vicinity of the corresponding threshold. Since the K^-d state is expected to have, similarly to K^-pp, rather large width, it is definitely out of this region.

It was demonstrated in [23] that increasing of the attraction in isospin-zero $\bar{K}N$ subsystem by hands (in the phenomenological antikaon-nucleon potentials only) leads to appearing of K^-d quasi-bound states. Therefore, the isospin-zero attraction in the $\bar{K}N$ system is not strong enough to bind antikaon to deuteron. It is necessary to note that the K^-d system with strong two-body interactions only is considered here. An atomic state caused by Coulomb interaction, kaonic deuterium, exists and will be considered later.

4.5 $\bar{K}\bar{K}N$ system: results

The calculations of the quasi-bound state in the $\bar{K}\bar{K}N$ system were performed with the two $\bar{K}\bar{K}$ interactions described in Section 2.4 (Original $V^{Orig}_{\bar{K}\bar{K}}$ and Lattice-motivated $V^{Latt}_{\bar{K}\bar{K}}$) and three $\bar{K}N$ potentials from Section 2.2: the phenomenological one-pole $V^{1,SIDD}_{\bar{K}N-\pi\Sigma}$ and two-pole $V^{2,SIDD}_{\bar{K}N-\pi\Sigma}$ phenomenological potentials together with the chirally-motivated potential $V^{Chiral}_{\bar{K}N-\pi\Sigma-\pi\Lambda}$. The results are presented in Table 3. It turned out that all combinations of the two-body interactions lead to a quasi-bound state in the three-body $\bar{K}\bar{K}N$ system. The quasi-bound state exists in the strangeness $S = -2$ system in spite of the repulsive character of the $\bar{K}\bar{K}$ interaction Comparison with the K^-pp characteristics from Table 2 shows that the quasi-bound state in the strangeness $S = -2$ $\bar{K}\bar{K}N$ system is much shallower and broader than the one in the $S = -1$ K^-pp system for the given $\bar{K}N$ potential.

Two methods of the quasi-bound state evaluation were used: the direct search method and the Breit-Wigner fit of the inverse determinant. It is seen from the Table 3 that the accuracy of the inverse

determinant method is much lower for the phenomenological $\bar{K}N$ interactions than for the chirally motivated one (and for the K^-pp system too). The reason is the larger widths of the "phenomenological" $\bar{K}\bar{K}N$ states, which means that the corresponding bumps are less pronounced, so they hardly can be fitted reliably by Breit-Wigner curves.

The found $\bar{K}\bar{K}N$ quasi-bound state has the same quantum numbers as a Ξ baryon with $J^P = (1/2)^+$. The available experimental information on the Ξ spectrum is rather limited, see PDG [28]. There is a $\Xi(1950)$ listed by the PDG, but its quantum numbers J^P are not determined, and it is unclear whether it should be identified with the quark-model state. It is possible that there are more than one resonance in this region. However, in spite of the fact, that the $\Xi(1950)$ state is situated above the $\bar{K}\bar{K}N$ threshold, four of the experimental values would be roughly consistent with the quasi-bound state found in the calculation [27]. Specifically, the experiment reported in Ref. [58] yielded a mass 1894 ± 18 MeV and a width 98 ± 23 MeV that is compatible with the range of values for the evaluated pole position.

An investigation on the $\bar{K}\bar{K}N$ system was also performed in [60], but several uncontrolled approximations were done there. In particular, energy-independent as well as energy-dependent potentials were used, but the two-body energy of the latter was fixed arbitrarily. Moreover, the imaginary parts of all complex potentials were completely ignored in the variational calculations in [60], the widths of the state were estimated separately. As a result, the binding energies are compared to the exact ones from [27], but the widths of the $\bar{K}\bar{K}N$ state are strongly underestimated.

5 Near-threshold K^-d scattering

5.1 Methods and exact results

The K^-pp quasi-bound state is a very interesting exotic object. However, it is not clear whether the accuracy of experimental results will be enough to draw some conclusions from comparison of the data with theoretical predictions. No strong quasi-bound state was found in the $\bar{K}NN$ system with other quantum numbers K^-d [23], but an atomic state, kaonic deuterium, exists, and its energy levels can be accurately measured. In addition, scattering of an antikaon on a deuteron can be studied.

Exact calculations of the near-threshold K^-d scattering were performed in [21; 23] using the three antikaon-nucleon potentials, described in Section 2.2, and different versions of the ΣN and NN potentials, described in Section 2.3. Namely, the exact optical and a simple complex versions of the spin-dependent and spin-independent $\Sigma N - \Lambda N$ potentials were used. The calculations were performed with TSA-A, TSA-B, and PEST models of the NN interaction.

The inhomogeneous system of the integral AGS equations, corresponding to Eq.(23) and describing the K^-d scattering, was transformed into the system of algebraic equations. It is known, that the original, one-channel, integral Faddeev equations have moving logarithmic singularities in the kernels when scattering above a three-body breakup threshold is considered. The K^-d amplitudes were calculated from zero up to the three-body breakup $\bar{K}NN$ threshold, so, in principle, the equations could be free of the singularities. However, the lower $\pi\Sigma N$ channel is opened when the K^-d scattering is considered, which causes appearance of the logarithmic singularities even below the three-body breakup $\bar{K}NN$ threshold. The problem was solved by interpolating of the unknown solutions in the singular region by certain polynomials and subsequent analytical integrating of the singular part of the kernels.

The K^-d scattering lengths a_{K^-d} obtained with the one- $V^{1,SIDD}_{\bar{K}N-\pi\Sigma}$ and two-pole $V^{2,SIDD}_{\bar{K}N-\pi\Sigma}$ versions of the phenomenological $\bar{K}N$ potential in [21] together with the chirally-motivated potential $V^{Chiral}_{\bar{K}N-\pi\Sigma-\pi\Lambda}$ in [23] are shown in Table 4. It is seen, that the chirally motivated potential leads to slightly larger absolute value of the real and the imaginary part of the scattering length than the phenomenological ones. However, the difference is small, so the three different models of the $\bar{K}N$ interaction, which reproduce the low-energy data on the K^-p scattering and kaonic hydrogen with the same level of accuracy, give quite similar results for low-energy K^-d scattering. It means that it is not possible to solve the question of the number of the poles forming the $\Lambda(1405)$ resonance from the results on the near-threshold elastic K^-d scattering.

The small difference between the "phenomenological" and "chiral" results of the a_{K^-d} calculations is opposite to the results obtained for the K^-pp system (see Section 4.2), where the binding energy and width of the K^-pp quasi-bound state were calculated using the same equations (the homogeneous ones

with properly changed quantum numbers, of cause) and input. In that case the three-body observables obtained with the three $\bar{K}N$ potentials turned out to be very different each from the other. The reason of this difference between the results for the near-threshold scattering and the quasi-bound state calculations could be the fact, that while the a_{K^-d} values were calculated near the $\bar{K}NN$ threshold, the K^-pp pole positions are situated far below it.

The amplitudes of the elastic K^-d scattering for kinetic energy from 0 to $E_{\rm deu}$, calculated using the three versions of the $\bar{K}N$ potential, are shown in Fig.3 of [21] and in Fig 5 of [23] in a form of $k\cot\delta(k)$ function. The chosen representation demonstrates that the elastic near-threshold K^-d amplitudes can be approximated by the effective range expansion rather accurately since the lines are almost straight. The calculated effective ranges $r^{\rm eff}_{K^-d}$ of the K^-d scattering, evaluated using the obtained K^-d amplitudes, are shown in Table 4.

The dependence of the full coupled-channel results on the NN and $\Sigma N(-\Lambda N)$ interaction models was investigated in [17]. The antikaon-nucleon phenomenological potentials, used there, reproduce the earlier KEK data on kaonic hydrogen and not the actual ones by SIDDHARTA. However, the results, obtained with those phenomenological $\bar{K}N$ potentials, are relative, so they must be valid for the actual potentials as well. In order to investigate dependence of the three-body results on the NN model of interaction, TSA-A, TSA-B, and PEST nucleon-nucleon potentials were used. It turned out that the difference for the K^-d scattering length is very small even for the potentials with and without repulsion at short distances (TSA and PEST, respectively). Therefore, the s-wave NN interaction plays a minor role in the calculations. Most likely, it is caused by the relative weakness of the NN interaction as compared to the $\bar{K}N$ one. Indeed, the quasi bound state in the latter system (which is the $\Lambda(1405)$ resonance with $E_{\bar{K}N}\approx -23$ MeV) is much deeper than the deuteron bound state ($E_{\rm deu}\approx 2$ MeV). Due to this, some visible effect from higher partial waves in NN is also not expected.

The dependence of a_{K^-d} on the $\Sigma N(-\Lambda N)$ interaction was also investigated in [17]. The K^-d scattering lengths were calculated with the exact optical and the simple complex versions of the spin dependent $V^{\rm Sdep}$ and spin independent $V^{\rm Sind}$ potentials. The results obtained with the two versions of the $\Sigma N(-\Lambda N)$ potential $V^{\rm Sdep}$ and $V^{\rm Sind}$ in exact optical form are very close, while their simple complex versions are slightly different. However, the largest error does not exceed 3%, therefore, the dependence of the K^-d scattering length a_{K^-p} on the $\Sigma N-(\Lambda N)$ interaction is also weak.

5.2 Approximate calculations and comparison to other results

It is hard to make a comparison with other theoretical results due to different methods and inputs used there. Due to this, several approximate calculations, in particular, one-channel $\bar{K}NN$ calculations with a complex and the exact optical $\bar{K}N$ potentials, were performed in [17]. In addition, a so-called FCA method was tested there.

In order to investigate the importance of the direct inclusion of the $\pi\Sigma N$ channel, the one-channel AGS calculations were performed in [17]. It means that Eq. (23) with $\alpha=\beta=1$ were solved, therefore, only the $\bar{K}N$ and NN T-matrices enter the equations. The exact optical and two simple complex one-channel $\bar{K}N(-\pi\Sigma)$ potentials approximating the full coupled-channel one- and two-pole phenomenological models of the interaction were used. As written in Section 2.2, the exact optical potential $V^{\rm Opt}$ provides exactly the same elastic $\bar{K}N$ amplitude as the coupled-channel model of the interaction. Its energy-dependent strength parameters are defined by Eq. (18) with $\bar{\alpha},\bar{\beta}=1,2$ stands for the $\bar{K}N$ and $\pi\Sigma$ channels, respectively.

The complex constants of the simple complex potentials were obtained in two ways. The first version of the simple complex $\bar{K}N$ potential reproduces the K^-p scattering length a_{K^-p} and the pole position z_1 of the corresponding coupled-channel version of the potentials. The second one gives the same isospin $I_i=0$ and $I_i=1$ $\bar{K}N$ scattering lengths as the full $\bar{K}N-\pi\Sigma$ potential.

It was found in [17] that the one-channel AGS calculation with the exact optical $\bar{K}N$ potential, giving exactly the same elastic $\bar{K}N$ amplitude as the corresponding coupled-channel phenomenological potential, is the best approximation. Its error does not exceed 2 percents. (The same is true for the results obtained with the chirally motivated $\bar{K}N$ potential, see [23].) On the contrary, the both simple complex $\bar{K}N$ potentials led to very inaccurate three-body results. Therefore, the one-channel Faddeev-type calculation with a simple complex antikaon-nucleon potential is not a good approximation for the low-energy elastic K^-d scattering.

One more approximate method, used for the a_{K^-d} calculations, is a so-called "Fixed center approximation to Faddeev equations" (FCA), introduced in [61]. In fact, it is a variant of FSA or a two-center formula. The fixed-scatterer approximation (FSA) or a two-center problem assumes, that the scattering of a projectile particle takes place on two much heavier target particles, separated by a fixed distance. The motion of the heavy particles is subsequently taken into account by averaging of the obtained projectile-target amplitude over the bound state wave function of the target. The approximation is well known and works properly in atomic physics, where an electron is really much lighter than a nucleon or an ion. Since the antikaon mass is just a half of the mass of a nucleon, it was expected, that FSA hardly can be a good approximation for the K^-d scattering length calculation.

The derivations of the FCA formula from Faddeev equations presented in [61] already rises questions, while the proper derivations of the FSA formula was done in [62]. The accuracy of the FCA was checked in [17] using the same input as in the AGS equations in order to make the comparison as adequate as possible.

First of all, the $\bar{K}N$ scattering lengths provided by the coupled-channel $\bar{K}N - \pi\Sigma$ potentials together with the deuteron wave function, corresponding to the TSA-B NN potential, were used in the FCA formula. Second, all $\bar{K}^0 n$ parts were removed from the formula because they drop off the AGS system of equations after the antisymmetrization. Finally, the fact, that the FCA formula was obtained for a local $\bar{K}N$ potential, while the separable $\bar{K}N - \pi\Sigma$ potentials were used in the Faddeev equations, was took into account, and the corresponding changes in the FCA formula were made.

The results of using of the FCA formula without "isospin-breaking effects" stay far away from the full calculation. While the errors for the imaginary part are not so large, the absolute value of the real part is underestimated by about 30%. Therefore, the calculations performed in [17] show that FCA is a poor approximation for the K^-d scattering length calculation. It is also seen from the figure that the accuracy is lower for the two-pole model of the $\bar{K}N$ interaction.

Therefore, among the approximate results the FCA was demonstrated to be the least accurate approximation, especially in reproducing of the real part of the K^-d scattering length. On the contrary, the one-channel AGS calculation with the exact optical $\bar{K}N(-\pi\Sigma)$ potential gives the best approximation to the full coupled-channel result. All approximations are less accurate for the two-pole phenomenological model of the $\bar{K}N - \pi\Sigma$ interaction.

Calculations of the K^-d scattering length were performed by other authors using Faddeev equations in [63; 64; 65; 66], while the FCA method was used in [61; 67]. The result of the very recent calculation with coupled channels [63] has real part of a_{K^-d}, which almost coincides with the result for chirally motivated potential shown in Table 4. The imaginary part of the K^-d scattering length from [63] is slightly larger. It might be caused by the fact that the model of the $\bar{K}N$ interaction, used there, was not fitted to the kaonic hydrogen data directly, but through the K^-p scattering length and the Deser-type approximate formula, which has larger error for the imaginary part of the level shift.

The two old a_{K^-d} values [65; 64], obtained within coupled-channel Faddeev approach, significantly underestimate the imaginary part of the K^-d scattering length, while their real parts are rather close to those in Table 4.

One more result of a Faddeev calculation [66] lies far away from all the others with very small absolute value of the real part of a_{K^-d}. One of the reasons is that the K^-d scattering length was obtained in [66] from one-channel Faddeev equations with a complex $\bar{K}N$ potential. However, the underestimation of the absolute value of its real part in comparison to other Faddeev calculations is so large, that it cannot be explained by the method only. The additional reason of the difference must be the $\bar{K}N$ potential, used in the paper. It gives so high position of the K^-p quasi bound state (1439 MeV), that it is situated above the K^-p threshold.

The a_{K^-d} values of [61] obtained using FCA method differ significantly from all other results. The absolute value of the real part of a_{K^-d} from [61] and its imaginary part are too large, which is caused by two factors. The first one is the FCA formula itself, which was shown to be inaccurate for the present system. The second reason are too large $\bar{K}N$ scattering lengths, used as the inputs.

The result of [67] was obtained by simple applying of two approximate formulas: FCA and the corrected Deser formula, used for calculation of the $\bar{K}N$ scattering lengths, entering the FCA. The values of [67] suffer not only from the cumulative errors from the two approximations, but from using of the DEAR results on kaonic hydrogen $1s$ level shift and width as well. Indeed, it was already written that the error of the corrected Deser formula makes about 10% for two-body case, the accuracy

of the FCA was shown to be poor. As for the problems with DEAR experimental data, they were demonstrated in [14] and in other theoretical works.

6 1s level shift of kaonic deuterium

The shift of the 1s level in the kaonic deuterium (which, strictly speaking, is the "antikaonic" deuterium) and its width are caused by the presence of the strong interactions in addition to the Coulomb one. It is a directly measurable value, which is free of a few uncertainties connected with an experiment on the K^-pp quasi-bound state. However, from theoretical point of view it is harder task due to necessity to take Coulomb potential into account directly together with the strong ones.

There are two ways to solve three-body problems accurately: solution of Faddeev equations or use of variational methods. However, for the case of an hadronic atom both methods face serious difficulties. The problem of the long range Coulomb force exists in the Faddeev approach, while variational methods suffer from the presence of two very different distance scales, which both are relevant for the calculations.

Due to this, at the first step the 1s level energy of the kaonic deuterium was calculated approximately using a two-body model of the atom. At the next step a method for simultaneous treatment of a short range plus Coulomb forces in three-body problems based on Faddeev equations [26] was used, and the lowest level of kaonic deuterium was calculated dynamically exactly.

6.1 Approximate calculation of kaonic deuterium 1s level

The approximate calculation of the kaonic deuterium was performed assuming that the atom can be considered as a two-body system consisting of a point-like deuteron, interacting with an antikaon through a complex strong $K^- - d$ potential and Coulomb. By this the size of a deuteron was taken into account only effectively through the strong potential, which reproduces the elastic three-body K^-d amplitudes, evaluated before. Keeping in mind the relative values of a deuteron and Bohr radius of the kaonic deuterium, the approximation seemed well grounded.

The complex two-body $K^- - d$ potential, constructed and used for investigation of the kaonic deuterium by Lippmann-Schwinger equation, is a two-term separable potential

$$V_{K^-d}(\mathbf{k},\mathbf{k}') = \lambda_{1,K^-d}\, g_1(\mathbf{k}) g_1(\mathbf{k}') + \lambda_{2,K^-d}\, g_2(\mathbf{k}) g_2(\mathbf{k}') \tag{31}$$

with Yamaguchi form-factors

$$g_i(k) = \frac{1}{\beta_{i,K^-d}^2 + k^2}, \qquad i = 1, 2. \tag{32}$$

The complex strength parameters λ_{1,K^-d} and λ_{2,K^-d} were fixed by the conditions, that the V_{K^-d} potential reproduces the K^-d scattering length a_{K^-d} and the effective range $r^{\rm eff}_{K^-d}$, obtained with one of the $\bar{K}N - \pi\Sigma$ potentials and presented in Table 4. A variation of the real β_{1,K^-d} and β_{2,K^-d} parameters allowed to reproduce the full near-threshold K^-d amplitudes from [21; 23] more accurately. As a result, the near-threshold amplitudes obtained from the three-body calculations $f^{(3)}_{K^-d}$ are reproduced by the two-body $K^- - d$ potentials through the interval $[0, E_{\rm deu}]$ with such accuracy, that the two-body functions $k\cot\delta^{(2)}(k)$ are indistinguishable from the three-body $k\cot\delta^{(3)}(k)$.

The parameters of the potentials are shown in Table 3 of [21] and in Eqs.(18,19) of [23]. Both β_{1,K^-d} and β_{2,K^-d} parameters for every $K^- - d$ potential are much smaller than the corresponding $\beta^{\bar{K}N}$ parameter of the $\bar{K}N$ potential. The constructed two-body complex potentials V_{K^-d} were used in the Lippmann-Schwinger equation. The calculations of the binding energy of a two-body system, described by the Hamiltonian with the strong and Coulomb interactions were performed in the same way as those of the K^-p system, see Section 2.2.

The shifts $\Delta E^{K^-d}_{1s}$ and widths $\Gamma^{K^-d}_{1s}$ of the 1s level of kaonic deuterium, corresponding to the three models of the $\bar{K}N$ interaction, described in Section 2.2, are shown in Table 4. It is seen that the "chirally motivated" absolute values of the level shift $\Delta E^{K^-d}_{1s}$ and the width $\Gamma^{K^-d}_{1s}$ are both slightly

Table 4 Scattering length a_{K^-d} (fm) and effective range $r^{eff}_{K^-d}$ (fm) of K^-d system obtained from AGS calculations with the one-pole $V^{1,SIDD}_{\bar{K}N-\pi\Sigma}$, two-pole $V^{2,SIDD}_{\bar{K}N-\pi\Sigma}$ phenomenological potentials and the chirally-motivated $V^{Chiral}_{\bar{K}N-\pi\Sigma-\pi\Lambda}$ potential. Approximate results for the $1s$ level shift $\Delta E^{K^-d}_{1s}$ (eV) and width $\Gamma^{K^-d}_{1s}$ (eV) of kaonic deuterium, corresponding to the AGS results on the near-threshold elastic amplitudes, are also shown.

$\bar{K}N$ potential used	a_{K^-d}	$r^{eff}_{K^-d}$	$\Delta E^{K^-d}_{1s}$	$\Gamma^{K^-d}_{1s}$
$V^{1,SIDD}_{\bar{K}N}$	$-1.49 + i\,1.24$	$0.69 - i\,1.31$	-785	1018
$V^{2,SIDD}_{\bar{K}N}$	$-1.51 + i\,1.25$	$0.69 - i\,1.34$	-797	1025
$V^{\rm Chiral}_{\bar{K}N}$	$-1.59 + i\,1.32$	$0.50 - i\,1.17$	-828	1055

larger than those obtained using the phenomenological $\bar{K}N - \pi\Sigma$ potentials. However, all three results do not differ one from the other more than several percents. It is similar to the case of the K^-d scattering length calculations, which turned out to be very close for the three $\bar{K}N$ potentials. The important point here is the fact that all three $\bar{K}N$ potentials reproduce the low-energy experimental data on K^-p scattering and kaonic hydrogen with the same level of accuracy. It is also important that the $1s$ level of kaonic deuterium is situated not far from the $\bar{K}NN$ threshold.

The closeness of the results for kaonic deuterium means that comparison of the theoretical predictions with eventual experimental results hardly could choose one of the models of the $\bar{K}N$ interaction, especially taking into account the large widths $\Delta E^{K^-d}_{1s}$. Therefore, it could not be possible to say, whether the potential of the antikaon-nucleon interaction should have one- or two-pole structure of the $\Lambda(1405)$ resonance and whether the potential should be energy dependent or not. It is seen from Tables 1 and 4 that there is no correlation between the pole or poles of the $\Lambda(1405)$ resonance given by a $\bar{K}N$ potential and the three-body K^-d elastic scattering or kaonic deuterium characteristics obtained using the potential.

Inaccuracy of the corrected Deser formula Eq.(10) was already shown for the two-body K^-p system, but some authors use it for the kaonic deuterium as well. Due to this, an accuracy of the formula was checked for this three-body system. The results were obtained using the a_{K^-d} values from Table 4. Being compared to the ΔE_{K^-d} and Γ_{K^-d} from the same table, the "corrected Deser" results show large error for all three versions of the antikaon-nucleon interaction. While difference for the shift is not so drastic, the width of the $1s$ level of the kaonic deuterium is underestimated by the corrected Deser formula by $\sim 30\%$.

The $1s$ level shift and width presented in Table 4 are not exact, they were evaluated using the two-body approximation, which, however, is well-grounded. Information on the three-body strong part is taken into account indirectly through the $K^- - d$ potential, reproducing the exact elastic K^-d amplitudes. On the contrary, the corrected Deser formula contains no three-body information at all since the only input is a K^-d scattering length, which is a complex number. Moreover, the formula relies on further approximations, which are absent in the accurate approximate calculations.

6.2 Exact calculation of kaonic deuterium: Faddeev equations with Coulomb interaction

Exact calculations of the kaonic deuterium were performed using a method [26] for simultaneous treatment of short range plus Coulomb forces in three-body problems, based on Faddeev equations. The method was successfully applied for purely Coulomb systems with attraction and repulsion and for the short range plus repulsive Coulomb forces. The case of an hadronic atom with three strongly interacting particles and Coulomb attraction between certain pairs was not considered before.

The basic idea of the method is to transform the Faddeev integral equations into a matrix form using a special discrete and complete set of Coulomb Sturmian functions as a basis. Written in coordinate space the Coulomb Sturmian functions are orthogonal with the weight function $1/r$. So that they form a bi-orthogonal and complete set with their counter-parts. The most remarkable feature of this particular set is, that in this representation the matrix of the two-body $(z - h^c)$ operator, where z is an energy and h^c is the pure two-body Coulomb Hamiltonian, is tridiagonal. When this property is used for evaluation of the matrix elements of the two-body Coulomb Green's function g^c, an infinite

tridiagonal set of equations, which can be solved exactly, is obtained. The same holds for the matrix elements of the free two-body Green's function g^0.

The system of equations with the Coulomb and strong interactions was solved in [25] for kaonic deuterium. This calculation is different from all other three-body calculations, described before. Already the initial form of the Faddeev equations for the kaonic deuterium differs from those for the pure strong interactions, described in Section 3. First, the equations should be written in coordinate space, while the AGS equations were written in momentum space. Second, since the Coulomb interaction acts between K^- and the proton, the particle basis was used and not the isospin one. Finally, the Faddeev equations with Coulomb do not define the transition operators, as e.g. those in Eq.(22), but the wave functions.

The equations are written in the Noble form [68], when the Coulomb interaction appears in the Green's functions. As usual for Faddeev-type equations, there are three partition channels $\alpha = (pn, K^-)$, (pK^-, n), (nK^-, p) and three sets of Jacobi coordinates. The system of homogeneous equations to be solved contains the matrix elements of the overlap between the basis functions from different Jacobi coordinate sets and of the strong potentials. They all can be calculated directly. The remaining parts of the kernel are matrix elements of the three-body partition Green's functions G_α. They are the basic quantities of the method, and their calculation depends on the partition channel.

The partition Green function $G_{(pK^-,n)}$ of the (pK^-, n) channel contains Coulomb interaction in its "natural" coordinate. It describes the (pK^-) subsystem and the neutron, which do not interact between themselves. Due to this, $G_{(pK^-,n)}$ can be calculated taking a convolution integral along a suitable contour in the complex energy plane over two two-body Green functions. As for the matrix elements of the two-body Green functions, they can be calculated using the properties of the Coulomb Sturmian basis and solving a resolvent equation.

The situation with the remaining G_α functions is more complicated. In the case of the $\alpha = (pn, K^-)$ and (nK^-, p) channels the Coulomb interaction is written not in its "natural" coordinates. Due to this, it should be rewritten as a sum of the Coulomb potential in the natural coordinates plus a short range potential U_α, which is a "polarization potential". The three-body Green function G^{ch}_α containing Coulomb potential in natural for the channel coordinates is called the "channel Green function", and it is evaluated similarly to the previous $\alpha = (pK^-, n)$ case. Namely, since the function describes a two-body subsystem and the non-interacting with it third particle, the $G^{ch}_{(pn,K^-)}$ and $G^{ch}_{(nK^-,p)}$ functions can be found by taking a convolution integral with two two-body Green's functions. At the last step the G_α function is found from the equation, containing the obtained channel Green function G^{ch}_α and the polarization potential U_α

$$G_\alpha(z) = G^{ch}_\alpha(z) + G^{ch}_\alpha(z) U_\alpha G_\alpha(z). \tag{33}$$

For the kaonic deuterium calculations it was necessary to take the isospin dependence of the $\bar{K}N$ interaction into account. In particle representation it means that the strong $V^s_{pK^-}$ potential is a 2×2 matrix, containing $V^s_{pK^-,pK^-}$, $V^s_{pK^-,n\bar{K}^0}$ and $V^s_{n\bar{K}^0,n\bar{K}^0}$ elements. Due to this, the final equations for the kaonic deuterium have four Faddeev components, including the additional one in the $(n\bar{K}^0, n)$ channel.

The solution of the Faddeev-type equations with Coulomb gave the full energy of the $1s$ level. Since the aim of [25] was evaluation of the $1s$ level shift of kaonic deuterium caused by the strong interactions between the antikaon and the nucleons, it was necessary to define the energy, from which the real part of the shift is measured. It can be the lowest eigenvalue of the channel Green function or of the "original" Green function of the (pn, K^-) channel. The first one corresponds to a deuteron and an antikaon feeling a Coulomb force from the center of mass of the deuteron. The second reflects the fact that the antikaon interacts via Coulomb force not with the center of the deuteron, but with the proton. In principle, the correct one should be the second variant, however, all approximate approaches use an analogy of the first one as the basic point, due to this it was used in [25] as well. In any case, the difference between both versions is small.

6.3 Exact calculation of kaonic deuterium: results

The calculation performed in [25] was considered as a first test of the method for the description of three-body hadronic atoms. Due to this, the second three-body particle channel $\pi\Sigma N$ was not directly

Table 5 Exact $1s$ level shifts ΔE (eV) and widths Γ (eV) of the kaonic deuterium for the four complex $\bar{K}N$ potentials V_I, V_{II}, V_{III}, and V_{IV}. The approximate results obtained using the corrected Deser formula and the complex $K^- - d$ potential are also shown.

	Corrected Deser		Complex $V_{K^- - d}$		Exact Faddeev	
	$\Delta_{1s}^{K^- d}$	$\Gamma_{1s}^{K^- d}$	$\Delta_{1s}^{K^- d}$	$\Gamma_{1s}^{K^- d}$	$\Delta_{1s}^{K^- d}$	$\Gamma_{1s}^{K^- d}$
V_I	-675	702	-650	868	-641	856
V_{II}	-694	740	-658	920	-646	888
V_{III}	-795	780	-747	1034	-732	980
V_{IV}	-750	620	-740	844	-736	826

included and no energy dependent potentials (exact optical or chirally motivated one) were used. The $\bar{K}N$ and NN interactions were described using one-term separable complex potentials with Yamaguchi form factors. Four versions of the $\bar{K}N$ potential V_I, V_{II}, V_{III} and V_{IV}, used in the calculations, give the $1s$ level shift of the kaonic hydrogen within or close to the SIDDHARTA data and a reasonable fit to the elastic $K^- p \to K^- p$ and charge exchange $K^- p \to \bar{K}^0 n$ cross-sections. Parameters of the potentials can be found in Table I of [25]. The nucleon-nucleon potential reproduces the NN scattering lengths, low-energy phase shifts and the deuteron binding energy in the np state.

The results of the dynamically exact calculations of the kaonic deuterium are presented in Table 5. The absolute values of the $1s$ level shift were found in the region $641 - 736$ eV, while the width variates between $826 - 980$ eV. Both observables are smaller than the accurate results from [23], shown in Table 4. However, it is necessary to remember that both calculations differ not only by the three-body methods, but also by the two-body input. To make the comparison reasonable, the two-body approximate calculation, described in Section 6.1, was repeated with the simple complex $\bar{K}N$ potentials V_I, V_{II}, V_{III}, and V_{IV}. The corrected Deser formula was also checked for these potentials. The approximate results are shown in Table 5.

It is seen that the two-body approximate calculation, described in Section 6.1, makes $\leq 2\%$ error for the shift and $\leq 5\%$ for the width, so it is quite accurate. It is an expected result keeping in mind the relative values of deuteron and Bohr radius of kaonic deuterium. The corrected Deser formula Eq.(10) leads to $2 - 8\%$ error in the shift, and strongly, up to 25%, underestimates the width.

It is also possible to compare the approximate results obtained in [25] with the four complex $\bar{K}N$ potentials V_I, V_{II}, V_{III}, and V_{IV} and in [23] with the coupled-channel models of the antikaon-nucleon interaction (the phenomenological $V_{\bar{K}N-\pi\Sigma}^{1,SIDD}$ and $V_{\bar{K}N-\pi\Sigma}^{2,SIDD}$ with one- and two-pole structure of the $\Lambda(1405)$ resonance respectively, and the chirally motivated $V_{\bar{K}N-\pi\Sigma-\pi\Lambda}^{Chiral}$). It is seen that the ''complex one-channel" absolute values of the $1s$ level shift and width shown in Table 5 are smaller than the ''coupled-channel" ones presented in Table 4. The similar situation was observed with the exactly evaluated characteristics of the strong pole in the $K^- pp$ system, while a one-channel simple complex antikaon - nucleon potential led to more narrow and less bound quasi-bound state than the coupled-channel version (see Eqs.(26,27)). But the differences for the kaonic deuterium are smaller than those for the $K^- pp$ quasi-bound state.

The very recent calculations [69] of the kaonic deuterium $1s$ level shift were performed using the same Faddeev-type equations with Coulomb interaction as in [25], but with energy-dependent $\bar{K}N$ potentials. Namely, the exact optical versions of the one- and two-pole phenomenological $\bar{K}N - \pi\Sigma$ potentials and of the chirally motivated $\bar{K}N - \pi\Sigma - \pi\Lambda$ interaction model were used. The predicted $1s$ level shifts (800 ± 30 eV) and widths (960 ± 40 eV) are larger by absolute value than the exact ones from Table 5 evaluated with the simple complex antikaon nucleon potentials.

Keeping in mind good accuracy of the results obtained with the exact optical $\bar{K}N$ potentials for all three-body $\bar{K}NN$ observables, demonstrated in the present paper, the predictions of [69] for the kaonic deuterium must be the most accurate ones up to date. The two-body approximation used in [21; 23], being compared to the more accurate approach of [69], gives very accurate value of the $1s$ level shift (the error is $\leq 2\%$), while the error for the width is larger ($\leq 9\%$).

7 Summary

The three-body antikaon nucleon systems could provide an important information about the antikaon nucleon interaction. It is quite useful since the two-body $\bar{K}N$ potentials of different type can reproduce all low-energy experimental data with the same level of accuracy. This fact was demonstrated on the example of the phenomenological $\bar{K}N - \pi\Sigma$ potentials with one and two-pole structure of the $\Lambda(1405)$ resonance together with the chirally motivated $\bar{K}N - \pi\Sigma - \pi\Lambda$ potential. Being used in the three-body calculations, the three $\bar{K}N$ potentials allowed to investigate the influence of the $\bar{K}N$ model on the results.

It was found that while the quasi-bound state position in the K^-pp and K^-K^-p systems strongly depends on the model of the $\bar{K}N$ interaction, the near-threshold observables (K^-d scattering length, elastic near-threshold K^-d amplitudes, $1s$ level shift and width of kaonic deuterium) are almost insensitive to it. Therefore, some conclusions on the number of poles of the $\Lambda(1405)$ resonance could be done only if a hight accuracy measurement of K^-pp binding energy and width will be done. Probably, one of the existing experiments: by HADES [9] and LEPS [10] collaborations, and in J-PARC [11; 12] hopefully will clarify the situation with the K^-pp quasi-bound state, - will do it. While dependence of the three-body results on the $\bar{K}N$ potentials is different for the different systems and processes, dependence on NN and ΣN interactions is weak in all cases.

Comparison of the exact results with some approximate ones revealed the most accurate approximations. In particular, the one-channel Faddeev calculations give results, which are very close to the coupled-channel calculations if the exact optical $\bar{K}N$ potential is used. This fact gives a hope for four-body calculations, which are already very complicated without additional coupled-channel structure. It is necessary to note here that the "exact optical" potential is defined as an energy dependent potential, which exactly reproduces the elastic amplitudes of the corresponding potential with coupled channels.

As for the kaonic deuterium, influenced mainly by Coulomb interaction, the shift of its $1s$ level caused by the strong interactions is described quite accurately in the two-body approximation. The $K^- - d$ complex potential should herewith reproduce the exact elastic three-body K^-d amplitudes, and the Lippmann-Schwinger equation must be solved exactly with Coulomb plus the strong potentials. Of cause, the exact calculation is more precise and, therefore, is preferable. The predicted by the exact calculations $1s$ level energy could be checked by SIDDHARTA-2 collaboration [70].

The suggested $1/|\mathrm{Det(z)}|^2$ method of theoretical evaluation of an underthreshold resonance is quite accurate for rather narrow and well pronounced resonances. It could supplement the direct search of the pole providing the first estimation and working as a control. The method is free from the uncertainties connected with the calculations on the complex plane, but it has the logarithmic singularities in the kernels of the integral equations.

The next step in the field of the few-body systems consisting of antikaons and nucleons should be done toward the four body systems. They could give more possibilities, but theoretical investigations of them are much more complicated.

References

1. Akaishi, Y., Yamazaki, T.: Nuclear $\bar{K}$ bound states in light nuclei. Phys. Rev. C 65, 044005 (2002)
2. Yamazaki, T., Akaishi, Y.: (K^-, π^-) production of nuclear $\bar{K}$ bound states in proton-rich systems via Λ^* doorways. Phys. Lett. B 535, 70 (2002)
3. Shevchenko, N.V., Gal, A., Mareš, J.: Faddeev calculation of a K^-pp quasi-bound state. Phys. Rev. Lett. 98, 082301 (2007)
4. Shevchenko, N.V., Gal, A., Mareš, J., Révai, J.: $\bar{K}NN$ quasi-bound state and the $\bar{K}N$ interaction: coupled-channel Faddeev calculations of the $\bar{K}NN - \pi\Sigma N$ system. Phys. Rev. C 76, 044004 (2007)
5. Ikeda, Y., Sato, T.: Strange dibaryon resonance in the $\bar{K}NN - \pi YN$ system. Phys. Rev. C 76, 035203 (2007)
6. Agnello, M. et al.: Evidence for a kaon-bound State K^-pp produced in K^- absorption reactions at rest. Phys. Rev. Lett. 94, 212303 (2005)
7. Bendiscioli, G. et al.: Search for signals of bound $\bar{K}$ nuclear states in antiproton -^{4}He annihilations at rest. Nucl. Phys. A 789, 222 (2007)
8. Yamazaki, T. et al.: Indication of a deeply bound and compact K^-pp state formed in the $pp \to p\Lambda K^+$ reaction at 2.85 GeV. Phys. Rev. Lett. 104, 132502 (2010)
9. Fabbietti, L. et. al.: $p\Lambda K^+$ final state: towards the extraction of the ppK^- contribution. Nucl. Phys. A 914, 60 (2013)

10. Tokiyasu, A.O. et al.: Search for the K^-pp bound state via $\gamma d \to K^+\pi^- X$ reaction at $E_\gamma = 1.5 - 2.4$ GeV. Phys. Lett. B 728, 616 (2014)
11. Ajimura, S. et al.: A search for deeply-bound kaonic nuclear state at the J-PARC E15 experiment. Nucl. Phys. A 914, 315 (2013)
12. Ichikawa, Y. et al.: J-PARC E27 experiment to search for a nuclear kaon bound state K^-pp. Few Body Syst. 54, 1191 (2013)
13. Révai, J., Shevchenko, N.V.: On extracting information about hadron-nuclear interaction from hadronic atom level shifts. Few Body Syst. 42, 83 (2008)
14. Révai, J., Shevchenko, N.V.: Isospin mixing effects in low-energy $\bar{K}N - \pi\Sigma$ interaction. Phys. Rev. C 79, 035202 (2009)
15. Cieplý, A., Smejkal, J.: Chirally motivated $\bar{K}N$ amplitudes for in-medium applications. Nucl. Phys. A 881, 115 (2012)
16. Oller, J.A., Meißner, U.-G.: Chiral dynamics in the presence of bound states: kaon-nucleon interactions revisited. Phys. Lett. B 500, 263 (2001)
17. Shevchenko, N.V.: One- versus two-pole $\bar{K}N - \pi\Sigma$ potential: K^-d scattering length. Phys. Rev. C 85, 034001 (2012)
18. Bazzi, M. *et al.* (SIDDHARTA Collaboration): A new measurement of kaonic hydrogen X-rays. Phys. Lett. B 704, 113 (2011)
19. Beer, G. et al.: Measurement of the kaonic hydrogen X-ray spectrum. Phys. Rev. Lett. 94, 212302 (2005)
20. Iwasaki, M. et al.: Observation of kaonic hydrogen K_α X rays. Phys. Rev. Lett. 78, 3067 (1997)
21. Shevchenko, N.V.: Near-threshold K^-d scattering and properties of kaonic deuterium. Nucl. Phys. A 890-891, 50-61 (2012)
22. Révai, J.: Signature of the $\Lambda(1405)$ resonance in neutron spectra from the $K^- + d$ reaction. Few Body Syst. 54, 1865-1876 (2013); Few Body Syst. 54, 1877 (2013)
23. Shevchenko, N.V., Révai, J.: Faddeev calculations of the $\bar{K}NN$ system with chirally-motivated $\bar{K}N$ interaction. I. Low-energy K^-d scattering and antikaonic deuterium. Phys. Rev. C 90, 034003 (2014)
24. Révai, J., Shevchenko, N.V.: Faddeev calculations of the $\bar{K}NN$ system with chirally-motivated $\bar{K}N$ interaction. II. The K^-pp quasi-bound state. Phys. Rev. C 90, 034004 (2014)
25. Doleschall, P., Révai, J., Shevchenko, N.V.: Three-body calculation of the $1s$ level shift in kaonic deuterium. Phys. Lett. B 744, 105-108 (2015)
26. Papp, Z., Plessas, W.: Coulomb-Sturmian separable expansion approach: Three-body Faddeev calculations or Coulomb-like interactions. Phys. Rev. C 54, 50 (1996)
27. Shevchenko, N.V., Haidenbauer, J.: Exact calculations of a quasibound state in the $\bar{K}\bar{K}N$ system. Phys. Rev. C 92, 044001 (2015)
28. Olive K.A. et al. (Particle Data Group): The Review of Particle Physics (2015). Chin. Phys. C, 38, 090001 (2014) and 2015 update
29. Ohnishi, S., Ikeda, Y., Hyodo, T., Hiyama, E., Weise, W.: $K^-d \to \pi\Sigma n$ reactions and structure of the (1405), J.Phys.Conf.Ser. 569 (2014) no.1, 012077; arXiv:1408.0118 [nucl-th]
30. Ohnishi, S., Ikeda, Y., Hyodo, T., Weise, W.: Structure of the (1405) and the $K^-d \to \pi\Sigma n$ reaction, Phys. Rev. C 93, 025207 (2016)
31. Moriya, K. (for the CLAS Collaboration): Measurement of the $\Sigma\pi$ photoproduction line shapes near the $\Lambda(1405)$. Phys. Rev. C 87, 035206 (2013)
32. Tovee, D.N. et al.: Some properties of the charged Σ hyperons. Nucl. Phys. B 33, 493 (1971)
33. Nowak, R.J. et al.: Charged Σ hyperon production by K^- meson interactions at rest. Nucl. Phys. B 139, 61 (1978)
34. Meißner, U.-G., Raha, U., Rusetsky, A.: Spectrum and decays of kaonic hydrogen. Eur. Phys. J. C 35, 349 (2004)
35. Sakitt, M. et al.: Low-energy K^--meson interactions in hydrogen. Phys. Rev. 139, B 719 (1965)
36. Kim, J.K.: Low-energy K^--p interaction and interpretation of the 1405-MeV Y_0^* resonance as a $\bar{K}N$ bound state. Phys. Rev. Lett. 14, 29 (1965)
37. Kim, J.K.: Multichannel phase-shift analysis of $\bar{K}N$ interaction in the region 0 to 550 MeV/c. Phys. Rev. Lett. 19, 1074 (1967)
38. Kittel, W., Otter, G., Wacek, I.: The K^- proton charge exchange interactions at low energies and scattering lengths determination. Phys. Lett. 21, 349 (1966)
39. Ciborowski, J. et al.: Kaon scattering and charged Sigma hyperon production in K^-p interactions below 300 MeV/c. J. Phys. G 8, 13 (1982)
40. Evans, D. et al.: Charge-exchange scattering in K^-p interactions below 300 MeV/c. J. Phys. G 9, 885 (1983)
41. Doleschall, P.: *private communication*
42. Wiringa, R.B., Stoks, V.G.J., Schiavilla, R.: Accurate nucleon-nucleon potential with charge-independence breaking. Phys. Rev. C 51, 38 (1995)
43. Zankel, H., Plessas, W., Haidenbauer, J.: Sensitivity of N-d polarization observables on the off-shell behavior of the N-N interaction. Phys. Rev. C 28, 538 (1983)
44. Alexander, G. et al.: Study of the $\Lambda - N$ system in low-energy $\Lambda - p$ elastic scattering. Phys. Rev. 173, 1452 (1968)

45. Sechi-Zorn, B., Kehoe, B., Twitty, J., Burnstein, R.A.: Low-energy Λ-proton elastic scattering. Phys. Rev. 175, 1735 (1968)
46. Eisele, F. et al.: Elastic $\Sigma^{\pm}p$ scattering at low energies. Phys. Lett. B 37, 204 (1971)
47. Engelmann, R., Filthuth, H., Hepp, V., Kluge, E.: Inelastic $\Sigma^{-}p$-interactions at low momenta. Phys. Lett. 21, 587 (1966)
48. Hepp, V., Schleich, M.: A new determination of the capture ratio $r_c = \frac{\Sigma^- p \to \Sigma^0 n}{(\Sigma^- p \to \Sigma^0 n) + (\Sigma^- p \to \Lambda^0 n)}$, the Λ^0-lifetime and the $\Sigma^- - \Lambda^0$ mass difference. Z. Phys. 214, 71 (1968)
49. Lohse, D., Durso, J.W., Holinde, K., Speth, J.: Meson exchange model for pseudoscalar meson-meson scattering. Nucl. Phys. A 516, 513 (1990)
50. Janssen, G., Pearce, B.C., Holinde, K., Speth, J.: Structure of the scalar mesons $f_0(980)$ and $a_0(980)$. Phys. Rev. D 52, 2690 (1995)
51. Beane, S.R. et al. (NPLQCD Collaboration): The K^+K^+ scattering length from lattice QCD. Phys. Rev. D 77, 094507 (2008)
52. Sasaki, K., Ishizuka, N., Oka, M., Yamazaki, T. (PACS-CS Collaboration): Scattering lengths for two pseudoscalar meson systems. Phys. Rev. D 89, 054502 (2014)
53. Alt, E.O., Grassberger, P., Sandhas, W.: Reduction of the three-particle collision problem to multi-channel two-particle Lippmann-Schwinger equations. Nucl. Phys. B 2, 167 (1967)
54. Ikeda, Y., Sato, T.: Energy Dependence of $\bar{K}NN$ Interactions and Resonance Pole of Strange Dibaryons. Prog. Theor. Phys. 124, 533 (2010)
55. Doté, A., Hyodo, T., Weise, W.: Variational calculation of the ppK^- system based on chiral SU(3) dynamics. Phys. Rev. C 79, 014003 (2009)
56. Barnea, N., Gal, A., Liverts, E.Z.: Realistic calculations of $\bar{K}NN$, $\bar{K}NNN$, and $\bar{K}\bar{K}NN$ quasibound states. Phys. Lett. B 712, 132 (2012)
57. Kezerashvili, R. Ya. et al: Three-body calculations for the K^-pp system within potential models. J. Phys. G: Nucl. Part. Phys. 43 (2016) 065104.
58. Dauber, P.M., Berge, J.P., Hubbard, J.R., Merrill, D.W., Muller, R.A.: Production and decay of cascade hyperons. Phys. Rev. 179, 1262 (1969)
59. Guo, L. et al.: Cascade production in the reactions $\gamma p \to K^+K^+(X)$ and $\gamma p \to K^+K^+\pi^-(X)$. Phys. Rev. C 76, 025208 (2007)
60. Kanada-En'yo, Y., Jido, D.: $\bar{K}\bar{K}N$ molecular state in three-body calculation. Phys. Rev. C 78, 025212 (2008)
61. Kamalov, S.S., Oset, E., Ramos, A.: Chiral unitary approach to the K^--deuteron scattering length. Nucl. Phys. A 690, 494 (2001)
62. Peresypkin, V.V.: Consideration of the recoil effect under a light particle scatteriing by two heavy particles. Ukr. Fiz. Zh. 23, 1256 (1978)
63. Mizutani, T., Fayard, C., Saghai, B., Tsushima, K.: Faddeev-chiral unitary approach to the K^-d scattering length. Phys. Rev. C 87, 035201 (2013)
64. Toker, G., Gal, A., Eisenberg, J.M.: The YN interactions and K^- reactions on deuterium at low energies. Nucl. Phys. A 362, 405 (1981)
65. Torres, M., Dalitz, R.H., Deloff, A.: K^- absorption reactions from rest in deuterium. Phys. Lett. B 174, 213 (1986)
66. Deloff, A.: $\eta - d$ and $K^- - d$ zero-energy scattering: A Faddeev approach. Phys. Rev. C 61, 024004 (2000)
67. Meissner, U.-G., Raha, U., Rusetsky, A.: Kaon-nucleon scattering lengths from kaonic deuterium experiments. Eur. Phys. J. C 47, 473 (2006)
68. Noble, J.V.: Three-body problem with charged particles. Phys. Rev. 161, 945 (1967)
69. Révai, J.: Three-body caculation of the $1s$ level shift in kaonic deuterium with realistic potentials. arXiv:1608.01802 [nucl-th]
70. Curceanu, C. et al.: Unlocking the secrets of the kaonnucleon/nuclei interactions at low-energies: The SIDDHARTA(-2) and the AMADEUS experiments at the DAΦNE collider. Nucl. Phys. A 914, 251 (2013)